III, 1

# APPENDIX 3

III, 2

# ICAO Aircraft Engine Emissions Databank

Civil Aviation Authority

**Contents**


1. Data Sources
2. Background
3. Revision of data
4. Contacts
5. Use of the Data Bank
6. Definitions
7. Regulatory standards
8. References


## 1. Data Sources

This Databank contains information on exhaust emissions of only those aircraft engines that have entered production. The information was provided by engine manufacturers, who are solely responsible for its accuracy. It was collected in the course of the work carried out by the ICAO Committee on Aviation Environmental Protection (CAEP) but has not been independently verified unless indicated. The UK CAA is hosting this Databank on behalf of ICAO and is not responsible for the contents.

## 2. Background

Standards limiting the emissions of smoke, unburnt hydrocarbons (HC), carbon monoxide (CO) and oxides of nitrogen ($NO_x$) from turbojet and turbofan aircraft engines are contained in Annex 16 Volume II (Second Edition, July 1993, plus amendments) [Reference 1] to the Convention on International Civil Aviation. The Annex also contains approved test and measurement procedures.

With respect to subsonic applications, the provisions of the Standards for smoke apply to engines whose date of manufacture is on or after 1 January 1983. For the gaseous emissions, the Standards apply only to engines whose rated output is greater than 26.7 kN. For hydrocarbons and carbon monoxide, they apply to engines whose date of manufacture is on or after 1 January 1986. For oxides of nitrogen, the Standards have several levels of stringency depending on the date of manufacture of the engine. These Standards are summarized later in Section 7.

This Databank contains information on exhaust emissions of only those engines that have entered production, irrespective of the numbers actually produced. It has been compiled mainly from information supplied for newly certified engines. However, for some engines, the data has been revised to reflect evidence from subsequent engine tests. It also includes data on older engines which did not have to comply with the emissions standards and some data from a very limited number of in-service engines measured before or after overhaul.

The original version was published as a printed document [Reference 2]. All subsequent updates have been electronic

## 3. Revision of data

The electronic version of the Databank is updated at periodic intervals. New data are included for:

a) engines certificated since the last issue of the data bank;
b) engines already certificated for which data were not previously available; or
c) engines already certificated and listed in the Databank for which:
   i. emissions data have been recalculated as a result of a better definition of engine performance characteristics with continuing production of an engine type;
   ii. component design changes have been introduced which affect the emissions levels, e.g. new combustor design; or
   iii. improvements in emissions measurement techniques have resulted in changes to the emissions data.

Data will not be removed from the Databank. Where data is superseded the row is marked to indicate that this data should not be used, and the newer data to be used instead is specified. Data is also marked where an engine is no longer in service, and where an engine is no longer in production.

The Record of Changes documents the history of revisions, and the date of latest review.

## 4. Contacts

New data should be submitted to:

Aircraft Environmental Section
Aircraft Certification Department
Safety Regulation Group
Civil Aviation Authority
Aviation House
Gatwick Airport South
West Sussex
RH6 0YR
United Kingdom

email: Emissions.Databank@srg.caa.co.uk
phone: (+44) 1293 573204

Comments and queries concerning this electronic version of the database should also be sent to the above address.

## 5. Use of the Databank

The user of the Databank should note the limitations in the emissions data; i.e.:

III, 4

a) The $D_p/F_{oo}$ values are based on an idealized Landing/Take-Off (LTO) cycle in International Standard Atmosphere (ISA) conditions. In assessing, for example, total aircraft emissions at a specific airport, consideration must be given to the appropriateness of the prescribed thrusts, the times in mode and the reference conditions.

b) The LTO cycle only assesses the emissions below 915 m (3 000 ft) and therefore may not be a good guide for comparing the emissions of different engines in other flight modes, e.g. cruise.

## 6. Definitions

*By-pass ratio:* The ratio of the air mass flow through the by-pass ducts of a gas turbine engine to the air mass flow through the engine core, calculated at maximum thrust when the engine is stationary in an international standard atmosphere at sea level.

*Characteristic level:* The characteristic level of a gaseous pollutant or smoke is the mean $D_p/F_{oo}$ or SN value of a species, for all the engines tested, measured and corrected to the reference standard engine and reference atmospheric conditions, divided by a coefficient corresponding to the number of engines tested. The procedure and coefficients are given in Annex 16, Volume II. This is in recognition that at the certification stage there are usually not many engines to production standard available for testing, so the manufacturer is allowed to select any number of engines, including a single engine if so desired, for testing. Statistically derived coefficients, corresponding to the number of engines tested, are then applied to ensure a high confidence that the mean of the anticipated total engine production will not exceed the regulatory level. The procedure and coefficients are given in Annex 16 Volume II, Appendix 6.

*Data Status:* This has been grouped into three categories:

1. *Pre-regulation:* Data obtained on engines generally prior to the promulgation of the Standards of Annex 16, Volume II, and for which the manufacturer was not required to apply for emissions certification.

2. *Certification:* Data which have been submitted for certification approval after the applicability dates or which have been obtained at an earlier date, generally after the promulgation of the Standards of Annex 16. Volume II, with the intention of gaining approval.

3. *Revised:* Existing data which have been modified, as noted in paragraph c) under REVISION OF DATA above, and which do not require the engine to be re-certificated.

*$D_p/F_{oo}$:* The mass, in grams ($D_p$), of any pollutant emitted during the reference landing and take-off (LTO) cycle, divided by the rated output ($F_{oo}$) of the engine.

*Emissions index (EI):* The mass of pollutant (CO, HC or $NO_x$), in grams, divided by the mass of fuel used in kilograms.

*Fuel:* The fuel used is aviation kerosene as specified in Annex 16, Volume II, Appendix 4.

*Hydrocarbons (HC):* The total of hydrocarbon compounds of all classes and molecular weights contained in a gas sample, calculated as if they were in the form of methane.

*International Standard Atmosphere (ISA):* The atmosphere defined in the Manual of the ICAO Standard Atmosphere (Doc 7488). These are the atmospheric conditions to which all engine performance data should be corrected.

*LTO cycle:* The reference emissions LTO cycle defines the thrust settings to be used when making emissions and smoke measurements and the time to be used for each mode in the subsequent calculations of $D_p$. These thrust settings and times are listed in Annex 16, Volume II, Part III, Chapter 2 (engines for subsonic propulsion).

*Oxides of nitrogen ($NO_x$):* The sum of the amounts of the nitric oxide and nitrogen dioxide contained in a gas sample calculated as if the nitric oxide were in the form of nitrogen dioxide.

*Pressure ratio ($\pi_{oo}$):* The ratio of the mean total pressure at the last compressor discharge plane of the compressor to the mean total pressure at the compressor entry plane when the engine is developing take-off thrust rating in ISA sea level static conditions.

*Rated output ($F_{oo}$):* The maximum thrust available for take-off under normal operating conditions at ISA sea level static conditions without the use of water injection as approved by the certificating authority. Thrust is expressed in kilonewtons.

*Reference Atmospheric Conditions:* The atmospheric conditions to which all emissions results should be corrected. The reference atmospheric conditions are ISA at sea level except that the reference absolute humidity shall be 0.00634 kg water/kg dry air.

*Regulatory Level:* The level below which the characteristic $D_p/F_{oo}$ or Smoke Number value for a pollutant species must fall in order to obtain certification approval. The regulatory levels reproduced from Annex 16, Volume II, Part III, Chapters 2 (subsonic engines) are given below in Section 7.

*Smoke Number (SN):* The dimensionless term quantifying smoke emissions. Smoke Number is calculated from the reflectance of a filter paper measured before and after the passage of a known volume of a smoke-bearing sample.

## 7. Regulatory standards

These applicability requirements and regulatory levels are those found in Annex 16, Volume II, Part III, Chapter 2 (subsonic engines) and are included for reference purposes only.

III, 6

**Smoke**

*Applicability*
The regulatory levels are applicable to engines whose date of manufacture is on or after 1 January 1983.

*Regulatory smoke number*
The characteristic level of the smoke number at any thrust setting, measured in accordance with Annex 16, Volume II, must not exceed 83.6 $(F_{oo})^{-0.274}$ or a value of 50, whichever is lower.

**Gaseous emissions**

*Applicability*
The regulatory levels apply to engines whose rated output is greater than 26.7kN and whose date of manufacture is on or after 1 January 1986 and as further specified for oxides of nitrogen.

*Regulatory levels*
The characteristic levels of the gaseous emissions measured over the LTO cycle in accordance with Annex 16, Volume II, must not exceed the following regulatory levels:

Hydrocarbons (HC): $D_p/F_{oo} = 19.6$

Carbon monoxide (CO): $D_p/F_{oo} = 118$

Oxides of nitrogen (NOx):

a) for engines of a type or model of which the date of manufacture of the first individual production model was on or before 31 December 1995 and for which the date of manufacture of the individual engine was on or before 31 December 1999:

$$D_p/F_{oo} = 40 + 2\pi_{oo}$$

b) for engines of a type or model of which the date of manufacture of the first individual production model was after 31 December 1995 or for which the date of manufacture of the individual engine was after 31 December 1999:

$$D_p/F_{oo} = 32 + 1.6\pi_{oo}$$

c) for engines of a type or model of which the date of manufacture of the first individual production model was after 31 December 2003:

1. for engines with a pressure ratio of 30 or less:

i. for engines with a maximum rated thrust of more than 89.0 kN:

III, 7

$D_p/F_{oo} = 19 + 1.6\pi_{oo}$

ii. for engines with a maximum rated thrust of more than 26.7 kN but not more than 89.0 kN:

$D_p/F_{oo} = 37.572 + 1.6\pi_{oo} - 0.2087F_{oo}$

2. for engines with a pressure ratio of more than 30 but less than 62.5:

i. for engines with a maximum rated thrust of more than 89.0 kN:

$D_p/F_{oo} = 7 + 2.0\pi_{oo}$

ii. for engines with a maximum rated thrust of more than 26.7 kN but not more than 89.0 kN:

$D_p/F_{oo} = 42.71 + 1.4286\pi_{oo} - 0.4013F_{oo} + 0.00642\pi_{oo} \times F_{oo}$

3) for engines with a pressure ratio of 62.5 or more:

$D_p/F_{oo} = 32 + 1.6\pi_{oo}$

d) for engines of a type or model of which the date of manufacture of the first individual production model was after 31 December 2007:

1) for engines with a pressure ratio of 30 or less:

i. for engines with a maximum rated thrust of more than 89.0 kN:

$D_p/F_{oo} = 16.72 + 1.4080\pi_{oo}$

ii. for engines with a maximum rated thrust of more than 26.7 kN but not more than 89.0 kN:

$D_p/F_{oo} = 38.5486 + 1.6823\pi_{oo} - 0.2453F_{oo} - 0.00308\ \pi_{oo} \times F_{oo}$

2) for engines with a pressure ratio of more than 30 but less than 82.6:

i. for engines with a maximum rated thrust of more than 89.0 kN:

$D_p/F_{oo} = -1.04 + 2.0\pi_{oo}$

ii. for engines with a maximum rated thrust of more than 26.7 kN but not more than 89.0 kN:

$D_p/F_{oo} = 46.1600 + 1.4286\pi_{oo} - 0.5303F_{oo} + 0.00642\pi_{oo} \times F_{oo}$

III, 8

3) for engines with a pressure ratio of 82.6 or more:

$$D_p/F_{oo} = 32 + 1.6\pi_{oo}$$

## 8. References


1. ICAO Annex 16 "International standards and recommended practices, Environmental protection", Volume II "Aircraft engine emissions", 2nd ed. (1993) plus amendments:

   | | |
   |---|---|
   | Amendment 3, | 20 March 1997; |
   | Amendment 4, | 4 November 1999; |
   | Amendment 5, | 24 November 2005 |

2. ICAO Engine Exhaust Emissions Databank, First Edition 1995, ICAO, Doc 9646- AN/943.

# ICAO ENGINE EXHAUST EMISSIONS DATA BANK

## SUBSONIC ENGINES

III, 9

ENGINE IDENTIFICATION: CFM56-3C-1
UNIQUE ID NUMBER: 1CM007
ENGINE TYPE: TF

BYPASS RATIO: 5.1
PRESSURE RATIO ($\pi_{oo}$): 25.5
RATED OUTPUT ($F_{oo}$) (kN): 104.6

REGULATORY DATA

| CHARACTERISTIC VALUE: | HC | CO | NOx | SMOKE NUMBER |
|---|---|---|---|---|
| $D_p/F_{oo}$ (g/kN) or SN | 4.3 | 65.7 | 53.1 | 9.9 |
| AS % OF ORIGINAL LIMIT | 21.7 % | 55.7 % | 58.3 % | 42.4 % |
| AS % OF CAEP/2 LIMIT (NOx) | | | 72.9 % | |
| AS % OF CAEP/4 LIMIT (NOx) | | | 88.8 % | |

DATA STATUS

- \- PRE-REGULATION
- \- CERTIFICATION
- x REVISED (SEE REMARKS)

TEST ENGINE STATUS

- x NEWLY MANUFACTURED ENGINES
- \- DEDICATED ENGINES TO PRODUCTION STANDARD
- \- OTHER (SEE REMARKS)

EMISSIONS STATUS

- x DATA CORRECTED TO REFERENCE (ANNEX 16 VOLUME II)

CURRENT ENGINE STATUS

(IN PRODUCTION, IN SERVICE UNLESS OTHERWISE NOTED)

- x OUT OF PRODUCTION (DATE: - )
- \- OUT OF SERVICE

MEASURED DATA

| MODE | POWER SETTING ($\%F_{oo}$) | TIME minutes | FUEL FLOW kg/s | EMISSIONS INDICES (g/kg) HC | CO | NOx | SMOKE NUMBER |
|---|---|---|---|---|---|---|---|
| TAKE-OFF | 100 | 0.7 | 1.154 | 0.03 | 0.9 | 20.7 | 7.7 |
| CLIMB OUT | 85 | 2.2 | 0.954 | 0.04 | 0.9 | 17.8 | 3.9 |
| APPROACH | 30 | 4.0 | 0.336 | 0.07 | 3.1 | 9.1 | 2.5 |
| IDLE | 7 | 26.0 | 0.124 | 1.42 | 26.8 | 4.3 | 2.3 |
| LTO TOTAL FUEL (kg) or EMISSIONS (g) | | | 448 | 287 | 5591 | 4810 | - |
| NUMBER OF ENGINES | | | | 1 | 1 | 1 | 1 |
| NUMBER OF TESTS | | | | 3 | 3 | 3 | 3 |
| AVERAGE $D_p/F_{oo}$ (g/kN) or AVERAGE SN (MAX) | | | | 2.76 | 53.5 | 45.8 | 7.7 |
| SIGMA ($D_p/F_{oo}$ in g/kN, or SN) | | | | 0.38 | 2.85 | 0.82 | 0.76 |
| RANGE ($D_p/F_{oo}$ in g/kN, or SN) | | | | 2.33-3.06 | 51.2-56.7 | 45.3-46.8 | 6.8-8.3 |

ACCESSORY LOADS

POWER EXTRACTION 0 (kW) AT - POWER SETTINGS
STAGE BLEED 0 % CORE FLOW AT - POWER SETTINGS

ATMOSPHERIC CONDITIONS

| | |
|---|---|
| BAROMETER (kPa) | 95.98-97.49 |
| TEMPERATURE (K) | 279 - 286 |
| ABS HUMIDITY (kg/kg) | .002-.009 |

FUEL

| | |
|---|---|
| SPEC | Jet A |
| H/C | 1.93 |
| AROM (%) | 16 |

MANUFACTURER: CFMI
TEST ORGANIZATION: CFM56 Evaluation Engineering
TEST LOCATION: Peebles Site IVD
TEST DATES: FROM 11 Nov 83 TO 14 Nov 83

REMARKS

1. Ref GE Report R84AEB579.
2. Engine S/N 692441.
3. Revised based on 3/89 production status cycle.

# ICAO ENGINE EXHAUST EMISSIONS DATA BANK

## SUBSONIC ENGINES

III, 10

| | | | |
|---|---|---|---|
| ENGINE IDENTIFICATION: | CF6-50C1, -C2 | BYPASS RATIO: | 4.3 |
| UNIQUE ID NUMBER: | 1GE007 | PRESSURE RATIO ($\pi_{oo}$): | 29.8 |
| ENGINE TYPE: | TF | RATED OUTPUT ($F_{oo}$) (kN): | 230.4 |

REGULATORY DATA

| CHARACTERISTIC VALUE: | HC | CO | NOx | SMOKE NUMBER |
|---|---|---|---|---|
| $D_p/F_{oo}$ (g/kN) or SN | 37.3 | 99.0 | 64.3 | 4.8 |
| AS % OF ORIGINAL LIMIT | 190.1 % | 83.9 % | 64.6 % | 25.5 % |
| AS % OF CAEP/2 LIMIT (NOx) | | | 80.7 % | |
| AS % OF CAEP/4 LIMIT (NOx) | | | 96.5 % | |

DATA STATUS

x PRE-REGULATION
\- CERTIFICATION
\- REVISED (SEE REMARKS)

TEST ENGINE STATUS

x NEWLY MANUFACTURED ENGINES
\- DEDICATED ENGINES TO PRODUCTION STANDARD
\- OTHER (SEE REMARKS)

EMISSIONS STATUS

x DATA CORRECTED TO REFERENCE (ANNEX 16 VOLUME II)

CURRENT ENGINE STATUS

(IN PRODUCTION, IN SERVICE UNLESS OTHERWISE NOTED)
x OUT OF PRODUCTION (DATE: - )
\- OUT OF SERVICE

MEASURED DATA

| MODE | POWER SETTING ($\%F_{oo}$) | TIME minutes | FUEL FLOW kg/s | EMISSIONS INDICES (g/kg) HC | CO | NOx | SMOKE NUMBER |
|---|---|---|---|---|---|---|---|
| TAKE-OFF | 100 | 0.7 | 2.487 | 0.6 | 0.5 | 36.3 | 4.1 |
| CLIMB OUT | 85 | 2.2 | 1.975 | 0.7 | 0.5 | 29.7 | 2.7 |
| APPROACH | 30 | 4.0 | 0.66 | 1 | 4.3 | 9.5 | 2.7 |
| IDLE | 7 | 26.0 | 0.215 | 21.8 | 61.8 | 3.6 | 4.5 |
| LTO TOTAL FUEL (kg) or EMISSIONS (g) | | | 859 | 7715 | 21591 | 14247 | - |
| NUMBER OF ENGINES | | | | 6 | 6 | 6 | 6 |
| NUMBER OF TESTS | | | | 6 | 6 | 6 | 6 |
| AVERAGE $D_p/F_{oo}$ (g/kN) or AVERAGE SN (MAX) | | | | 33.5 | 93.7 | 61.8 | 4.5 |
| SIGMA ($D_p/F_{oo}$ in g/kN, or SN) | | | | 3.8 | 4.6 | 0.5 | 1.5 |
| RANGE ($D_p/F_{oo}$ in g/kN, or SN) | | | | - | - | - | - |

ACCESSORY LOADS

POWER EXTRACTION 0 (kW) AT - POWER SETTINGS
STAGE BLEED 0 % CORE FLOW AT - POWER SETTINGS

ATMOSPHERIC CONDITIONS

| | |
|---|---|
| BAROMETER (kPa) | 98.3-100.4 |
| TEMPERATURE (K) | 270 - 296 |
| ABS HUMIDITY (kg/kg) | .0027-.0103 |

FUEL

| | |
|---|---|
| SPEC | Jet A |
| H/C | 1.92 |
| AROM (%) | 17.1 |

MANUFACTURER: GE Aircraft Engines
TEST ORGANIZATION: Production Engine Test
TEST LOCATION: Production Test Cells M34 & M35
TEST DATES: FROM 12 Oct 79 TO 05 Dec 79

REMARKS

Ref Report no FAA-EE-80-27 (GE Report R80AEG420)

# ICAO ENGINE EXHAUST EMISSIONS DATA BANK

## SUBSONIC ENGINES

** DATA SUPERSEDED ** SEE SHEET: 8PW089

III, 11

ENGINE IDENTIFICATION: PW4084
UNIQUE ID NUMBER: 2PW062
ENGINE TYPE: TF

BYPASS RATIO: 6.4
PRESSURE RATIO ($\pi_{oo}$): 36.2
RATED OUTPUT ($F_{oo}$) (kN): 369.6

REGULATORY DATA

| CHARACTERISTIC VALUE: | HC | CO | NOx | SMOKE NUMBER |
|---|---|---|---|---|
| $D_p/F_{oo}$ (g/kN) or SN | 4.5 | 23.0 | 72.8 | 13.5 |
| AS % OF ORIGINAL LIMIT | 23.0 % | 19.5 % | 64.8 % | 81.6 % |
| AS % OF CAEP/2 LIMIT (NOx) | | | 81.0 % | |
| AS % OF CAEP/4 LIMIT (NOx) | | | 91.7 % | |

DATA STATUS

- PRE-REGULATION
x CERTIFICATION
- REVISED (SEE REMARKS)

TEST ENGINE STATUS

- NEWLY MANUFACTURED ENGINES
x DEDICATED ENGINES TO PRODUCTION STANDARD
- OTHER (SEE REMARKS)

EMISSIONS STATUS

x DATA CORRECTED TO REFERENCE (ANNEX 16 VOLUME II)

CURRENT ENGINE STATUS

(IN PRODUCTION, IN SERVICE UNLESS OTHERWISE NOTED)

- OUT OF PRODUCTION
- OUT OF SERVICE

MEASURED DATA

| MODE | POWER SETTING (%$F_{oo}$) | TIME minutes | FUEL FLOW kg/s | EMISSIONS INDICES (g/kg) HC | CO | NOx | SMOKE NUMBER |
|---|---|---|---|---|---|---|---|
| TAKE-OFF | 100 | 0.7 | 3.411 | 0.1 | 0.1 | 45 | 10.5 |
| CLIMB OUT | 85 | 2.2 | 2.689 | 0.1 | 0.1 | 35.5 | - |
| APPROACH | 30 | 4.0 | 0.875 | 0.2 | 0.4 | 12 | - |
| IDLE | 7 | 26.0 | 0.242 | 2.7 | 18.73 | 4.4 | - |
| LTO TOTAL FUEL (kg) or EMISSIONS (g) | | | 1086 | 1111 | 7205 | 23229 | - |
| NUMBER OF ENGINES | | | | 1 | 1 | 1 | 1 |
| NUMBER OF TESTS | | | | 3 | 3 | 3 | 3 |
| AVERAGE $D_p/F_{oo}$ (g/kN) or AVERAGE SN (MAX) | | | | 2.9 | 19.5 | 62.8 | 10.5 |
| SIGMA ($D_p/F_{oo}$ in g/kN, or SN) | | | | - | - | - | - |
| RANGE ($D_p/F_{oo}$ in g/kN, or SN) | | | | - | - | - | - |

ACCESSORY LOADS

POWER EXTRACTION 0 (kW) AT - POWER SETTINGS
STAGE BLEED 0 % CORE FLOW AT - POWER SETTINGS

ATMOSPHERIC CONDITIONS

| | |
|---|---|
| BAROMETER (kPa) | 101.3 |
| TEMPERATURE (K) | 288 |
| ABS HUMIDITY (kg/kg) | 0.0063 |

FUEL

| | |
|---|---|
| SPEC | Jet A |
| H/C | 1.92 |
| AROM (%) | 20.3 |

MANUFACTURER: Pratt and Whitney
TEST ORGANIZATION: Pratt and Whitney
TEST LOCATION: East Hartford, Ct, USA
TEST DATES: FROM 26 Apr 94 TO 02 May 94

REMARKS

Data from X832-4

If REVISED, this data supersedes databank UID 8PW090
Compliance with fuel venting requirements: - ('x' if complies, PR if pre-regulation)

# ICAO ENGINE EXHAUST EMISSIONS DATA BANK

## SUBSONIC ENGINES

III, 12

ENGINE IDENTIFICATION: JT3D-3B
UNIQUE ID NUMBER: 1PW001
ENGINE TYPE: TF

BYPASS RATIO: 1.4
PRESSURE RATIO ($\pi_{oo}$): 13.6
RATED OUTPUT ($F_{oo}$) (kN): 80.06

REGULATORY DATA

| CHARACTERISTIC VALUE: | HC | CO | NOx | SMOKE NUMBER |
|---|---|---|---|---|
| $D_p/F_{oo}$ (g/kN) or SN | 395.4 | 328.2 | 37.7 | 63.9 |
| AS % OF ORIGINAL LIMIT | 2,017.6 % | 278.2 % | 56.1 % | 254.1 % |
| AS % OF CAEP/2 LIMIT (NOx) | | | 70.2 % | |
| AS % OF CAEP/4 LIMIT (NOx) | | | 88.3 % | |

DATA STATUS

x PRE-REGULATION
- CERTIFICATION
- REVISED (SEE REMARKS)

TEST ENGINE STATUS

- NEWLY MANUFACTURED ENGINES
x DEDICATED ENGINES TO PRODUCTION STANDARD
- OTHER (SEE REMARKS)

EMISSIONS STATUS

x DATA CORRECTED TO REFERENCE (ANNEX 16 VOLUME II)

CURRENT ENGINE STATUS

(IN PRODUCTION, IN SERVICE UNLESS OTHERWISE NOTED)
x OUT OF PRODUCTION (DATE: - )
- OUT OF SERVICE

MEASURED DATA

| MODE | POWER SETTING ($\%F_{oo}$) | TIME minutes | FUEL FLOW kg/s | EMISSIONS INDICES (g/kg) HC | CO | NOx | SMOKE NUMBER |
|---|---|---|---|---|---|---|---|
| TAKE-OFF | 100 | 0.7 | 1.174 | 4 | 1.5 | 12.1 | - |
| CLIMB OUT | 85 | 2.2 | 0.932 | 2 | 2.8 | 9.9 | - |
| APPROACH | 30 | 4.0 | 0.346 | 4 | 24.5 | 4.8 | - |
| IDLE | 7 | 26.0 | 0.135 | 112 | 98 | 2.5 | - |
| LTO TOTAL FUEL (kg) or EMISSIONS (g) | | | 466 | 24363 | 23092 | 2740 | - |
| NUMBER OF ENGINES | | | | 2 | 2 | 2 | 2 |
| NUMBER OF TESTS | | | | - | - | - | - |
| AVERAGE $D_p/F_{oo}$ (g/kN) or AVERAGE SN (MAX) | | | | 303.9 | 288.1 | 34.3 | 54.5 |
| SIGMA ($D_p/F_{oo}$ in g/kN, or SN) | | | | - | - | - | - |
| RANGE ($D_p/F_{oo}$ in g/kN, or SN) | | | | - | - | - | - |

ACCESSORY LOADS

POWER EXTRACTION 0 (kW) AT - POWER SETTINGS
STAGE BLEED 0 % CORE FLOW AT - POWER SETTINGS

ATMOSPHERIC CONDITIONS

| | |
|---|---|
| BAROMETER (kPa) | - |
| TEMPERATURE (K) | - |
| ABS HUMIDITY (kg/kg) | - |

FUEL

| | |
|---|---|
| SPEC | Jet A |
| H/C | - |
| AROM (%) | - |

MANUFACTURER: Pratt & Whitney
TEST ORGANIZATION: P&WA
TEST LOCATION: East Hartford, CT, USA.
TEST DATES: FROM 08 Mar 72 TO 12 Sep 74

REMARKS

Emissions data estimated from JT3D-7 engines using JT3D-3B performance data.

IV, 1

# APPENDIX 4

IV, 2



# WMO Meteorological codes

*This document gives details of the Meteorological codes for use at observing stations.*

## Type / Genus of cloud:

*WMO code 0500:* **Genus of cloud**

/ - cloud not visible owing to darkness, fog, duststorm, sandstorm or other analogous phenomena
0 - cirrus (CI)
1 - cirricumulus (CC)
2 - cirrostratus (CS)
3 - altocumulus (AC)
4 - altostratus (AS)
5 - nimbostratus (NS)
6 - stratocumulus (SC)
7 - stratus (ST)
8 - cumulus (CU)
9 - cumulonimbus (CB)

## High cloud type:

*WMO code 0509:* **Clouds of genera Cirrus, Cirrocumulus and Cirrostratus.**

/ - cirrus, cirrocumulus & cirrostratus invisible owing to darkness, fog, blowing dust or sand, or other phenomena, or more often because of the presence of a continuous layer of lower clouds
0 - no cirrus, cirrocumulus or cirrostratus clouds
1 - cirrus in the form of filaments, strands or hooks, not progressively invading the sky.
2 - dense cirrus, in patches or entangled sheaves, which usually do not increase & sometimes seem to be the remains of the upper part of a cumulonimbus; or cirrus with sproutings in the form of small turrets; or cirrus having the appearance of cumuliform tufts
3 - dense cirrus, often in the form of an anvil, being the remains of the upper part of cumulonimbus
4 - cirrus in the form of hooks, filaments, or both, progressively invading the sky; they generally become denser as a whole.
5 - cirrus (often in bands converging towards 1 point or 2 opposite points of the horizon) and cirrostratus, or cirrostratus alone;in either case, they are progressively invading the sky, and generally growing denser as a whole, but the continuous veil does not reach 45 degrees above the horizon.
6 - cirrus (often in bands converging towards 1 point or 2 opposite points of the horizon) and cirrostratus, or cirrostratus alone;in either case, they are progressively invading the sky, and generally growing denser as a whole; the continuous veil extends more than 45 degrees above the horizon, without the sky being totally covered.
7 - veil of cirrostratus covering the celestial dome
8 - cirrostratus not progressively invading the sky and not completely covering the celestial dome.
9 - cirrocumulus alone, or cirrocumulus accompanied by cirrus or cirrostratus, or both, but cirrocumulus is predominant

## Low cloud type:

*WMO code 0513:* **Clouds of genera Stratocumulus, Stratus, Cumulus, etc.**

/ - stratocumulus, stratus, cumulus and cumulonimbus invisible owing to darkness, fog, blowing dust or sand, or other phenomena
0 - no stratocumulus, stratus, cumulus or cumulonimbus
1 - cumulus with little vertical extent and seemingly flattened, or ragged cumulus, other than of bad weather, or both
2 - cumulus of moderate or strong vertical extent, generally with protuberances in the form of domes or towers, either accompanied or not by other cumulus or stratocumulus, all having bases at the same level
3 - cumulonimbus, the summits of which, at least partially, lack sharp outlines but are neither clearly fibrous (cirriform) nor in the form of an anvil; cumulus, stratocumulus or stratus may also be present
4 - stratocumulus formed by the spreading out of cumulus; cumulus may also be present
5 - stratocumulus not resulting from the spreading out of cumulus
6 - stratus in a more or less continuous later, or in ragged shreds, or both but no stratus fractus of bad weather
7 - stratus fractus of bad weather or cumulus fractus of bad weather, or both (pannus), usually below altostratus or nimbostratus
8 - cumulus and stratocumulus other than that formed from the spreading out of cumulus; the base of the cumulus is at a different level from that of the stratocumulus
9 - cumulonimbus, the upper part of which is clearly fibrous (cirriform) often in the form of an anvil; either accompanied or not by cumulonimbus without anvil or fibrous upper part, by cumulus, stratocumulus, stratus or pannus

## Medium cloud type:

*WMO code 0515:* **Clouds of the genera Altocumulus, Altostratus, etc.**

/ - altocumulus, altostratus and nimbostratus invisible owing to darkness, fog,

IV, 3

blowing dust, sand, or other phenomena; or because of the presence of a continuous layer of lower clouds
0 - no altocumulus, altostratus or nimbostratus
1 - altostratus, the greater part of which is semi-transparent; through this part the sun or moon may be weakly visible, as through ground glass
2 - altostratus, the greater part of which is sufficiently dense to hide the sun or moon, or nimbostratus
3 - altocumulus, the greater part of which is semi-transparent; the various elements of the cloud change only slowly and are all at a single level
4 - patches (often in the form of almonds or fish) of altocumulus, the greater part of which is semi-transparent; the clouds occur at one or more levels and the elements are continually changing in appearance
5 - semi-transparent altocumulus in bands, or altocumulus, in one or more continuous layer (semi-transparent or opaque), progressively invading the sky; these generally thicken as a whole
6 - altocumulus resulting from the spreading out of cumulus or cumulonimbus
7 - altocumulus in two or more layers, usually opaque in places, and not progressively invading the sky; or opaque layer of altocumulus,not progressively invading the sky; or altocumulus together with altostratus or nimbostratus
8 - altocumulus with sproutings in the form of small towers or battlements, or altocumulus having the appearance of cumuliform tufts
9 - altocumulus of a chaotic sky, generally at several levels

## State of ground:

*WMO code 0901:* **State of ground without snow or measurable ice cover.**

0 - ground dry (no cracks or appreciable amounts of dust/loose sand)
1 - ground moist
2 - ground wet (standing water in small or large pools on surface)
3 - flooded
4 - ground frozen
5 - glaze on ground
6 - loose dry dust or sand not covering ground completely
7 - thin cover of loose dry dust or sand covering ground completely
8 - mod/thick cover of loose dry dust/sand covering ground completely
9 - extremely dry with cracks

*WMO code 0975:* **State of ground with snow or measurable ice cover.**

0 - ground predominantly covered by ice
1 - compact/wet snow (with or without ice) covering less than 1/2 the ground
2 - compact/wet snow (with or without ice) covering at least 1/2 the ground
3 - even layer of compact or wet snow covering ground completely
4 - uneven layer of compact or wet snow covering ground completely
5 - loose dry snow covering less than 1/2 the ground
6 - loose dry snow covering at least 1/2 the ground (not completely)
7 - even layer of loose dry snow covering ground completely
8 - uneven layer or loose dry snow covering ground completely
9 - snow covering ground completely; deep drifts

## Total cloud amount:

*WMO code 2700:* **Cloud cover / amount**

/ - cloud is indiscernible for reasons other than fog or other meteorological phenomena, or observation is not made.
0 - sky clear
1 - 1 okta : 1/10 - 2/10
2 - 2 oktas : 2/10 - 3/10
3 - 3 oktas : 4/10
4 - 4 oktas : 5/10
5 - 5 oktas : 6/10
6 - 6 oktas : 7/10 - 8/10
7 - 7 oktas or more, but not 8 oktas : 9/10 or more, but not 10/10
8 - 8 oktas : 10/10
9 - sky obscured by fog or other meteorological phenomena

## Past weather:

Past weather is defined as weather occurring in the past 6 hours at 00, 06, 12, 18 UTC, and the past 3 hours at 03, 09, 15, 21 UTC.

*WMO code 4561:* **Past weather**

0 - cloud covering half or less of the sky throughout the period
1 - cloud covering more than half the sky during part of the period & half or less for the rest
2 - cloud covering more than half the sky throughout the period
3 - sandstorm, duststorm or blowing snow
4 - fog or ice fog or thick haze
5 - drizzle
6 - rain
7 - snow, or rain and snow mixed
8 - shower(s)
9 - thunderstorm(s) with or without precipitation

## Present weather:

*WMO code 4677:* **Present weather reported from a manned station.**

00 - Cloud development not observed or not observable

IV, 4

01 - Cloud generally dissolving or becoming less developed
02 - State of sky on the whole unchanged
03 - Clouds generally forming or developing
04 - Visibility reduced by smoke, e.g. veldt or forest fires, industrial smoke or volcanic ashes
05 - Haze
06 - Widespread dust in suspension in the air, not raised by wind at or near the station at the time of observation
07 - Dust or sand raised by wind at or near the station at the time of observation, but not well-developed dust whirl(s) or sand whirl(s), and no duststorm or sandstorm seen; or, in the case of ships, blowing spray at the station
08 - Well-developed dust or sand whirl(s) seen at or near the station during the preceding hour or at the time of observation, but no dust storm or sandstorm
09 - Duststorm or sandstorm within sight at the time of observation, or at the station during the preceding hour
10 - Mist
11 - Patches of shallow fog or ice fog at the station, whether on land or sea not deeper than about 2 metres on land or 10 metres at sea
12 - More or less continuous shallow fog or ice fog at the station, whether on land or sea, not deeper than about 2m/land or 10m/sea
13 - Lightning visible, or thunder heard
14 - Precipitation within sight, not reaching the ground or the surface of the sea
15 - Precipitation within sight, reaching the ground or the surface of the sea, but distant, i.e. > 5 km from the station
16 - Precipitation within sight, reaching the ground or the surface of the sea, near to, but not at the station
17 - Thunderstorm, but no precipitation at the time of observation
18 - Squalls at or within sight of the station during the preceding hour or at the time of observation
19 - Funnel clouds at or within sight of the station during the preceding hour or at the time of observation
20 - Drizzle (not freezing) or snow grains, not falling as showers, during the preceding hour but not at the time of observation
21 - Rain (not freezing), not falling as showers, during the preceding hour but not at the time of observation
22 - Snow, not falling as showers, during the preceding hour but not at the time of observation
23 - Rain and snow or ice pellets, not falling as showers; during the preceding hour but not at the time of observation
24 - Freezing drizzle or freezing rain; during the preceding hour but not at the time of observation
25 - Shower(s) of rain during the preceding hour but not at the time of observation
26 - Shower(s) of snow, or of rain and snow during the preceding hour but not at the time of observation
27 - Shower(s) of hail, or of rain and hail during the preceding hour but not at the time of observation
28 - Fog or ice fog during the preceding hour but not at the time of observation
29 - Thunderstorm (with or without precipitation) during the preceding hour but not at the time of observation
30 - Slight or moderate duststorm or sandstorm - has decreased during the preceding hour
31 - Slight or moderate duststorm or sandstorm - no appreciable change during the preceding hour
32 - Slight or moderate duststorm or sandstorm - has begun or has increased during the preceding hour
33 - Severe duststorm or sandstorm - has decreased during the preceding hour
34 - Severe duststorm or sandstorm - no appreciable change during the preceding hour
35 - Severe duststorm or sandstorm - has begun or has increased during the preceding hour
36 - Slight/moderate drifting snow - generally low (below eye level)
37 - Heavy drifting snow - generally low (below eye level)
38 - Slight/moderate blowing snow - generally high (above eye level)
39 - Heavy blowing snow - generally high (above eye level)
40 - Fog or ice fog at a a distance at the time of observation, but not at station during the preceding hour, the fog or ice fog extending to a level above that of the observer
41 - Fog or ice fog in patches
42 - Fog/ice fog, sky visible, has become thinner during the preceding hour
43 - Fog/ice fog, sky invisible, has become thinner during the preceding hour
44 - Fog or ice fog, sky visible, no appreciable change during the past hour
45 - Fog or ice fog, sky invisible, no appreciable change during the preceding hour
46 - Fog or ice fog, sky visible, has begun or has become thicker during preceding hour
47 - Fog or ice fog, sky invisible, has begun or has become thicker during the preceding hour
48 - Fog, depositing rime, sky visible
49 - Fog, depositing rime, sky invisible
50 - Drizzle, not freezing, intermittent, slight at time of ob.
51 - Drizzle, not freezing, continuous, slight at time of ob.
52 - Drizzle, not freezing, intermittent, moderate at time of ob.
53 - Drizzle, not freezing, continuous, moderate at time of ob.
54 - Drizzle, not freezing, intermittent, heavy at time of ob.
55 - Drizzle, not freezing, continuous, heavy at time of ob.
56 - Drizzle, freezing, slight
57 - Drizzle, freezing, moderate or heavy (dense)
58 - Rain and drizzle, slight
59 - Rain and drizzle, moderate or heavy
60 - Rain, not freezing, intermittent, slight at time of ob.
61 - Rain, not freezing, continuous, slight at time of ob.
62 - Rain, not freezing, intermittent, moderate at time of ob.
63 - Rain, not freezing, continuous, moderate at time of ob.
64 - Rain, not freezing, intermittent, heavy at time of ob.
65 - Rain, not freezing, continuous, heavy at time of ob.
66 - Rain, freezing, slight
67 - Rain, freezing, moderate or heavy
68 - Rain or drizzle and snow, slight
69 - Rain or drizzle and snow, moderate or heavy
70 - Intermittent fall of snowflakes, slight at time of ob.
71 - Continuous fall of snowflakes, slight at time of ob.
72 - Intermittent fall of snowflakes, moderate at time of ob.
73 - Continuous fall of snowflakes, moderate at time of ob.
74 - Intermittent fall of snowflakes, heavy at time of ob.
75 - Continuous fall of snowflakes, heavy at time of ob.
76 - Diamond dust (with or without fog)
77 - Snow grains (with or without fog)

IV, 5

78 - Isolated star-like snow crystals (with or without fog)
79 - Ice pellets
80 - Rain shower(s), slight
81 - Rain shower(s), moderate or heavy
82 - Rain shower(s), violent
83 - Shower(s) of rain and snow, slight
84 - Shower(s) of rain and snow, moderate or heavy
85 - Snow shower(s), slight
86 - Snow shower(s), moderate or heavy
87 - Shower(s) of snow pellets or small hail, with or without rain or rain and snow mixed - slight
88 - Shower(s) of snow pellets or small hail, with or without rain or rain and snow mixed - moderate or heavy
89 - Shower(s) of hail, with or without rain or rain and snow mixed, not associated with thunder - slight
90 - Shower(s) of hail, with or without rain or rain and snow mixed, not associated with thunder - moderate or heavy
91 - Slight rain at time of observation - Thunderstorm during the preceding hour but not at time of observation
92 - Moderate or heavy rain at time of observation - Thunderstorm during the preceding hour but not at time of observation
93 - Slight snow, or rain and snow mixed or hail at time of observation - Thunderstorm during the preceding hour but not at time of observation
94 - Moderate or heavy snow, or rain and snow mixed or hail at time of observation - Thunderstorm during the preceding hour but not at time of observation
95 - Thunderstorm, slight or moderate, without hail, but with rain and/or snow at time of observation
96 - Thunderstorm, slight or moderate, with hail at time of ob.
97 - Thunderstorm, heavy, without hail, but with rain and/or snow at time of observation
98 - Thunderstorm combined with dust/sandstorm at time of observation
99 - Thunderstorm, heavy with hail at time of observation

## Pressure characteristic over last 3 hours:

*WMO code 0200:***Characteristic of pressure tendency.**

0 - Increasing, then decreasing ; atmospheric pressure the same as or higher than 3 hrs ago
1 - Increasing, then steady ; atmospheric preasure now higher than 3 hrs ago
2 - Increasing (steadily or unsteadily) ; atmospheric pressure now higher than 3 hrs ago
3 - Decreasing or steady, then increasing; or increasing, then increasing more rapidly ; atmospheric pressure now higher than 3 hrs ago
4 - Steady ; atmospheric pressure the same as 3 hrs ago
5 - Decreasing, then increasing ; atmospheric pressure the same as or lower than 3 hrs ago
6 - Decreasing, then steady; or decreasing then decreasing more slowly ; atmospheric pressure now lower than 3 hrs ago
7 - Decreasing (steadily or unsteadily) ; atmospheric pressure now lower than 3 hrs ago
8 - Steady or increasing, then decreasing; or decreasing, then decreasing more rapidly ; atmospheric pressure now lower than 3 hrs ago

## Day of Thunder:

6000 NCM table 24

0 - no thunderstorm (0000-2400gmt)
1 - thunderstorm with or without precipitation
9 - no thunderstorm (restricted period)

## Day of Hail:

6001 NCM table 23

0 - no hail,ice,etc (0000-2400gmt)
1 - diamond dust
2 - snow grains
3 - snow pellets
4 - ice pellets or small hail (less than 5mm dianeter)
5 - hail ( diameter 5-9 mm)
6 - hail ( diameter 10-19 mm)
7 - hail ( diameter 20mm or more )
9 - no hail ,ice etc restricted period

## Day of snow or sleet:

6002 NCM table 27

0 - no snow or sleet(0000-2400gmt)
1 - sleet
5 - snow
9 - no snow or sleet(restricted period)

## Day of fog:

6003 NCM table 25

0 - visibility 1000m or more at 0900 gmt(previous day)
1 - visibility less than 1000m at 0900 gmt

IV, 6

**Day of Gale:**

6004 NCM table 26

0 - no gale(0000-2400 gmt)
1 - day on which wind speed has reached 34 knots (beaufort force 8) for a period of at least 10 minutes
9 - no gale (restricted period)

**State of concrete:**

6005 NCM table 22

/ - slab covered by snow or not adequately described by codes 0 to 3
0 - slab dry
1 - slab moist
2 - slab wet
3 - slab icy

**Snow lying at 0900GMT:**

6006 CDN flag

0 - no snow or less than half cover of snow lying
1 - more than half cover of snow at 0900z today

**Snow depth:**

001 - 1cm
002 - 2cm
... - ...
996 - 996cm
997 - Less than 0.5cm
998 - Snow cover, not continuous
999 - Measurement impossible or inaccurate

020011 CLOUD AMOUNT

0 0
1 1 OKTA OR <1
2 2 OKTAS
3 3 OKTAS
4 4 OKTAS
5 5 OKTAS
6 6 OKTAS
7 7 OKTAS (<8)
8 8 OKTAS
9 SKY OBSCURED METEOROLOGICAL
10 SKY PARTLY OBSCURED BY FOG AND/OR OTHER METEOROLOGICAL PHENOMENA
11 SCATTERED
12 BROKEN
13 FEW

020012 CLOUD TYPE

0 CI
1 CC
2 CS
3 AC
4 AS
5 NS
6 SC
7 ST
8 CU
9 CB
10 NO CH CLOUDS
11 CI FIB (UNC)
12 CI SPI SHEAF
13 CI SPI CUGEN
14 CI UNC/FIB
15 CI VEIL <45°
16 CI VEIL >45°
17 CS WHOLE SKY
18 CS NOT COVER
19 CH MOSTLY CC
20 NO CM CLOUDS
21 AS TR
22 AS OP / NS
23 AC TR LEVEL
24 AC TR PATCHY
25 AC TR BANDS
26 AC CU(CB)GEN
27 AC TR LAYERS
28 AC CAS/FLO
29 AC CHAOTIC
30 NO CL CLOUDS
31 CU HUM/FRA
32 CU MED/CON
33 CU CAL
34 SC CUGEN
35 SC NOT CUGEN
36 SC NEB/FRA
37 ST/CU FRA
38 CU/SC LEVELS

IV, 7

```
39 CB CAP
40
41
42
43
44
45
46
47
48
49
50
51
52
53
54
55
56
57
58
59 CLOUD INVIS
60 CH INVISIBLE
61 CM INVISIBLE
62 CL INVISIBLE
```

Home Contact Disclaimer Last Modified: Wed, 25 Apr 2007 10:55:59 GMT

V, 1

# APPENDIX 5

# Updated Aviation Radiative Forcing for 2000

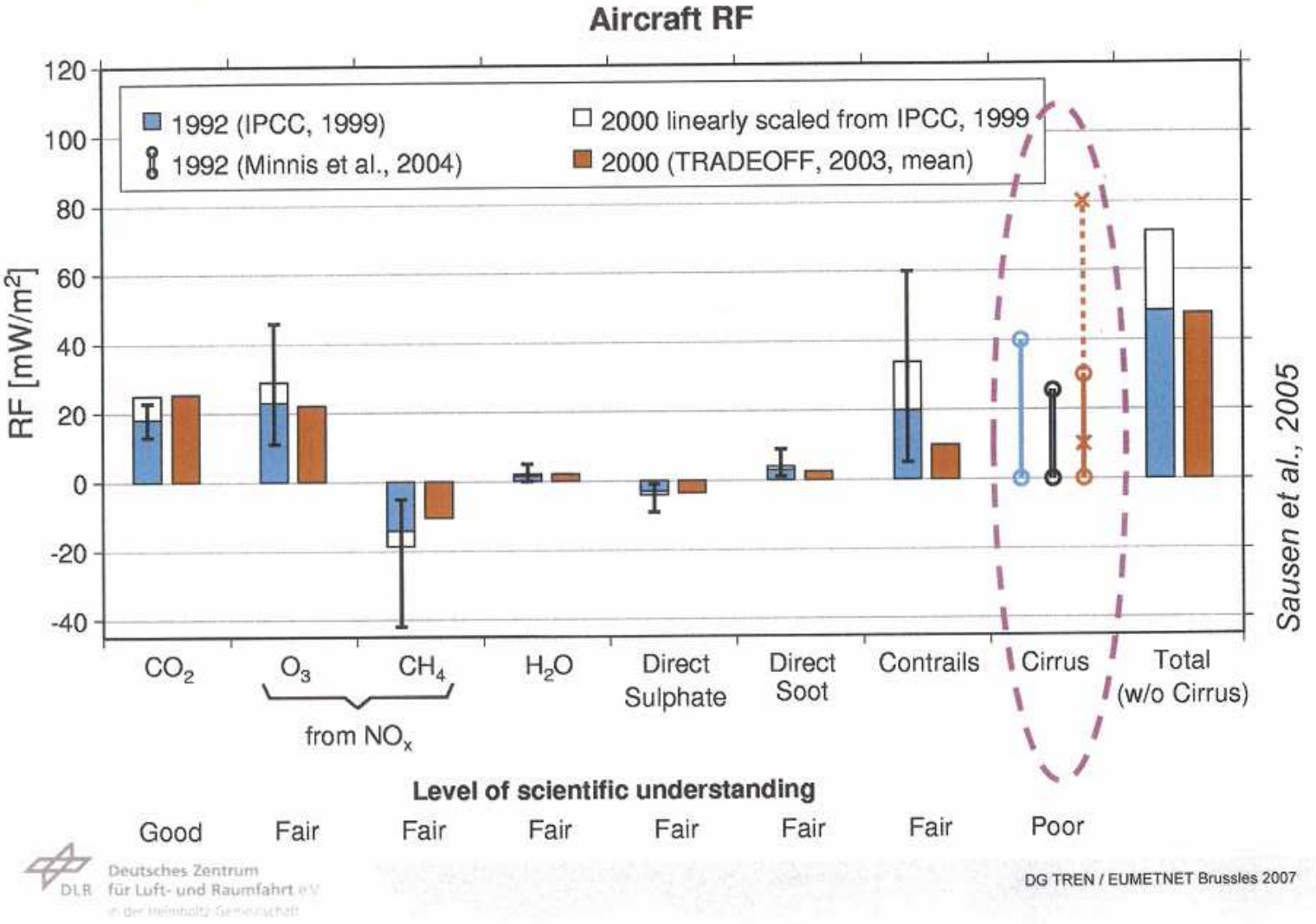


Deutsches Zentrum für Luft- und Raumfahrt e.V. in der Helmholtz-Gemeinschaft

DG TREN / EUMETNET Brussles 2007

03.05.2007

17

VI, (

# APPENDIX 6

VI, 2



# Contrails reduce daily temperature range

A brief interval when the skies were clear of jets unmasked an effect on climate.

The potential of condensation trails (contrails) from jet aircraft to affect regional-scale surface temperatures has been debated for years[1–3], but was difficult to verify until an opportunity arose as a result of the three-day grounding of all commercial aircraft in the United States in the aftermath of the terrorist attacks on 11 September 2001. Here we show that there was an anomalous increase in the average diurnal temperature range (that is, the difference between the daytime maximum and night-time minimum temperatures) for the period 11–14 September 2001. Because persisting contrails can reduce the transfer of both incoming solar and outgoing infrared radiation[4,5] and so reduce the daily temperature range, we attribute at least a portion of this anomaly to the absence of contrails over this period.

We analysed maximum and minimum temperature data[6] from about 4,000 weather stations throughout the conterminous United States (the 48 states not including Alaska and Hawaii) for the period 1971–2000, and compared these to the conditions that prevailed during the three-day aircraft-grounding period. All sites were inspected for data quality and adjusted for the time of observation.

Because the grounding period commenced after the minimum temperatures had been reached on the morning of 11 September and ended before maximum temperatures were attained on 14 September (at noon, Eastern Standard Time), we staggered the calculation of the average diurnal temperature range (DTR) across adjacent days (for example, 11 September maxima minus 12 September minima). We repeated this procedure for the three-day periods immediately before and after the grounding period, and also for the same periods (8–11, 11–14 and 14–17 September) for each year from 1971 to 2000.

DTRs for 11–14 September 2001 measured at stations across the United States show an increase of about 1.1 °C over normal 1971–2000 values (Fig. 1). This is in contrast to the adjacent three-day periods, when DTR values were near or below the mean (Fig. 1). DTR departures for the grounding period are, on average, 1.8 °C greater than DTR departures for the two adjacent three-day periods.

This increase in DTR is larger than any during the 11–14 September period for the previous 30 years, and is the only increase greater than 2 standard deviations away from the mean DTR (s.d., 0.85 °C). Moreover, the 11–14 September increase in DTR

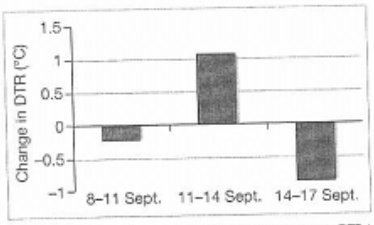


**Figure 1** Departure of average diurnal temperature ranges (DTRs) from the normal values derived from 1971–2000 climatology data for the indicated three-day periods in September 2001. These periods included the three days before the terrorist attacks of 11 September; the three days immediately afterwards, when aircraft were grounded and there were therefore no contrails; and the subsequent three days.

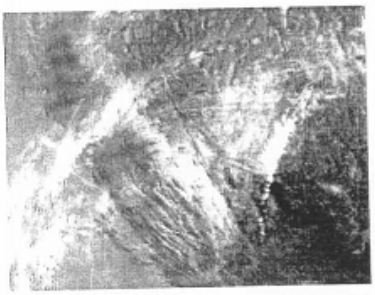

NOAA SATELLITE ACTIVE ARCHIVE

**Figure 2** Flight lines: jet contrails can clearly be seen as thin streaks in this satellite image of the southwestern United States.

was more than twice the national average for regions of the United States where contrail coverage has previously been reported to be most abundant (such as the midwest, northeast and northwest regions)[7].

Day-to-day changes in synoptic atmospheric conditions can affect regional DTRs[8]. In particular, a lack of cloud cover helps to increase the maximum (and reduce the minimum) temperature. Maps of the daily average outgoing long-wave radiation (OLR)[9,10] — a proxy for optically thick clouds — show reduced cloudiness (that is, larger OLR) over the eastern half of the United States on 11 September, but more cloud (smaller OLR) over parts of the west. Cloud cover subsequently decreased in the west and increased over much of the eastern half of the country during the next two days, producing predominantly negative three-day OLR changes in the east and positive values in parts of the west.

Our findings indicate that the diurnal temperature range averaged across the United States was increased during the aircraft-grounding period, despite large variations in the amount of cloud associated with mobile weather systems (Fig. 2). We argue that the absence of contrails was responsible for the difference between a period of above-normal but unremarkable DTR and the anomalous conditions that were recorded.

**David J. Travis*, Andrew M. Carleton†, Ryan G. Lauritsen***

**Department of Geography and Geology, University of Wisconsin–Whitewater, Whitewater, Wisconsin 53190, USA*
*e-mail: travisd@.uww.edu*
*†Department of Geography, Pennsylvania State University, University Park, Pennsylvania 16801, USA*

1. Changnon, S. A. *J. Appl. Meteorol.* **20**, 496–508 (1981).
2. Travis, D. J. & Changnon, S. A. *J. Weather Modification* **29**, 74–83 (1997).
3. Sassen, K. *Bull. Am. Meteorol. Soc.* **78**, 1885–1903 (1997).
4. Duda, D. P., Minnis, P. & Nguyen, L. *J. Geophys. Res.* **106**, 4927–4937 (2001).
5. Meerkotter, R. *et al. Ann. Geophys.* **17**, 1080–1094 (1999).
6. National Oceanic and Atmospheric Administration. *TD3200/3210 Data Set for 1971–2001* (Natl Climate Data Center, Asheville, North Carolina, 2001).
7. DeGrand, J. Q., Carleton, A. M., Travis, D. J. & Lamb, P. J. *Appl. Meteorol.* **39**, 1434–1459 (2000).
8. Karl, T. R. *et al. Bull Am. Meteorol. Soc.* **74**, 1007–1023 (1993).
9. Liebmann, B. & Smith, C. A. *Bull Am. Meteorol. Soc.* **77**, 1275–1277 (1996).
10. http://www.cdc.noaa.gov (NOAA-CIRES Climate Diagnostics Center, Boulder, Colorado, USA).

**Competing financial interests:** declared none.

Animal behaviour

## Male parenting of New Guinea froglets

Male parental care is exceptionally rare in nature, although one of the most fascinating aspects of New Guinea's biodiversity is the evolution of male care in the frog family Microhylidae[1]. Here I report a new mode of parental care: transport of froglets by the male parent, which was recently discovered in two species of microhylid frogs from the mountains of Papua New Guinea. As the offspring jump off at different points, they may benefit from reduced competition for food, lower predation pressure and fewer opportunities for inbreeding between froglets, which may explain why this unusual form of parental care evolved.

I quantified the parental care behaviour of several species of microhylid frog at the Crater Mountain Biological Research Station, Chimbu Province, Papua New Guinea (6° 43′ S, 145° 05′ E), which is located on the largest tropical island in

VI, 3



# Regional Variations in U.S. Diurnal Temperature Range for the 11–14 September 2001 Aircraft Groundings: Evidence of Jet Contrail Influence on Climate

DAVID J. TRAVIS

*Department of Geography and Geology, University of Wisconsin—Whitewater, Whitewater, Wisconsin*

ANDREW M. CARLETON

*Department of Geography and Environment Institute, The Pennsylvania State University, University Park, Pennsylvania*

RYAN G. LAURITSEN

*Department of Geography, Northern Illinois University, Dekalb, Illinois*

(Manuscript received 26 November 2002, in final form 3 September 2003)

ABSTRACT

The grounding of all commercial aircraft within U.S. airspace for the 3-day period following the 11 September 2001 terrorist attacks provides a unique opportunity to study the potential role of jet aircraft contrails in climate. Contrails are most similar to natural cirrus clouds due to their high altitude and strong ability to efficiently reduce outgoing infrared radiation. However, they typically have a higher albedo than cirrus; thus, they are better at reducing the surface receipt of incoming solar radiation. These contrail characteristics potentially suppress the diurnal temperature range (DTR) when contrail coverage is both widespread and relatively long lasting over a specific region. During the 11–14 September 2001 grounding period natural clouds and contrails were noticeably absent on high-resolution satellite imagery across the regions that typically receive abundant contrail coverage. A previous analysis of temperature data for the grounding period reported an anomalous increase in the U.S.-averaged, 3-day DTR value. Here, the spatial variation of the DTR anomalies as well as the separate contributions from the maximum and minimum temperature departures are analyzed. These analyses are undertaken to better evaluate the role of jet contrail absence and synoptic weather patterns during the grounding period on the DTR anomalies.

It is shown that the largest DTR increases occurred in regions where contrail coverage is typically most prevalent during the fall season (from satellite-based contrail observations for the 1977–79 and 2000–01 periods). These DTR increases occurred even in those areas reporting positive departures of tropospheric humidity, which may reduce DTR, during the grounding period. Also, there was an asymmetric departure from the normal maximum and minimum temperatures suggesting that daytime temperatures responded more to contrail absence than did nighttime temperatures, which responded more to synoptic conditions. The application of a statistical model that "retro-predicts" contrail-favored areas (CFAs) on the basis of upper-tropospheric meteorological conditions existing during the grounding period, supports the role of contrail absence in the surface temperature anomalies; especially for the western United States. Along with previous studies comparing surface climate data at stations beneath major flight paths with those farther away, the regionalization of the DTR anomalies during the September 2001 "control" period implies that contrails have been helping to decrease DTR in areas where they are most abundant, at least during the early fall season.

## 1. Introduction

An important consideration in identifying the climate impacts of changes in cloud radiative forcing are the role of high clouds, including the "false cirrus" condensation trails (contrails) generated by jet aircraft. Contrails may persist as "outbreaks" on multihour (3–6 h) time scales and over space scales of more than 1000 km$^2$ (Travis et al. 1997; Penner et al. 1999; Minnis et al. 2002). These contrail outbreaks may obscure a substantial portion of the sky or mix with "natural" cirrus to enhance the total cloud amount (Bakan et al. 1994; Travis et al. 1997; Duda et al. 2001; Fig. 1). Hence, the radiative forcing produced by contrails may be significant for those regions of the United States characterized by many such outbreaks (e.g., the Midwest, parts of the West Coast, the Northeast and Southeast; Minnis et al. 1997; Sassen 1997; DeGrand et al. 2000).

Some researchers have speculated that persisting contrails exacerbate "global warming" in areas where they

*Corresponding author address:* Dr. David J. Travis, Department of Geography and Geology, University of Wisconsin—Whitewater, Whitewater, WI 53190.
E-mail: travisd@uww.edu

FIG. 1. AVHRR thermal IR (band 4) image (at 1.1-km resolution) of a contrail "outbreak" over the Midwest taken at 1000 UTC 11 Sep 1995. The southern tip of Lake Michigan can be seen at the top of the image.

most frequently occur, due to their ability to reduce outgoing infrared radiation while transmitting some solar radiation to the surface; similar to natural cirrus (e.g., Meerkotter et al. 1999). However, there is probably a diurnal dependence to the role of contrails in radiative forcing that is missing in the case of natural cirrus, and that is enhanced by the strong diurnal variability of aircraft flight frequencies. Because contrails contain a higher density of relatively small ice crystals compared with natural cirrus clouds (Murcray 1970; Gothe and Grassl 1993), the contrail radiative forcing during daylight hours may be dominated by the higher albedo of contrails versus natural cirrus, leading to a potential surface "cooling" (Mims and Travis 1997). At night, the infrared forcing of contrails dominates relative to clear-sky conditions, producing a surface "warming" effect similar to natural clouds. Thus, when considered across a 24-h period it is possible that the net contrail radiative forcing is relatively small. However, the combination of both the daytime cooling and nighttime warming effects should result in a decrease in the diurnal temperature range (DTR), as shown in previous case studies (e.g., Travis and Changnon 1997; Travis et al. 2002). Thus, a need exists to investigate the net effect of contrails on surface temperature across a range of geographic regions and synoptic conditions, especially because significant decreases in DTR have been reported for some areas of the United States during the second half of the twentieth century, including those where contrails are most abundant (e.g., Karl et al. 1993; Travis and Changnon 1997).

Previous attempts to identify a contrail effect in the

VI, 5



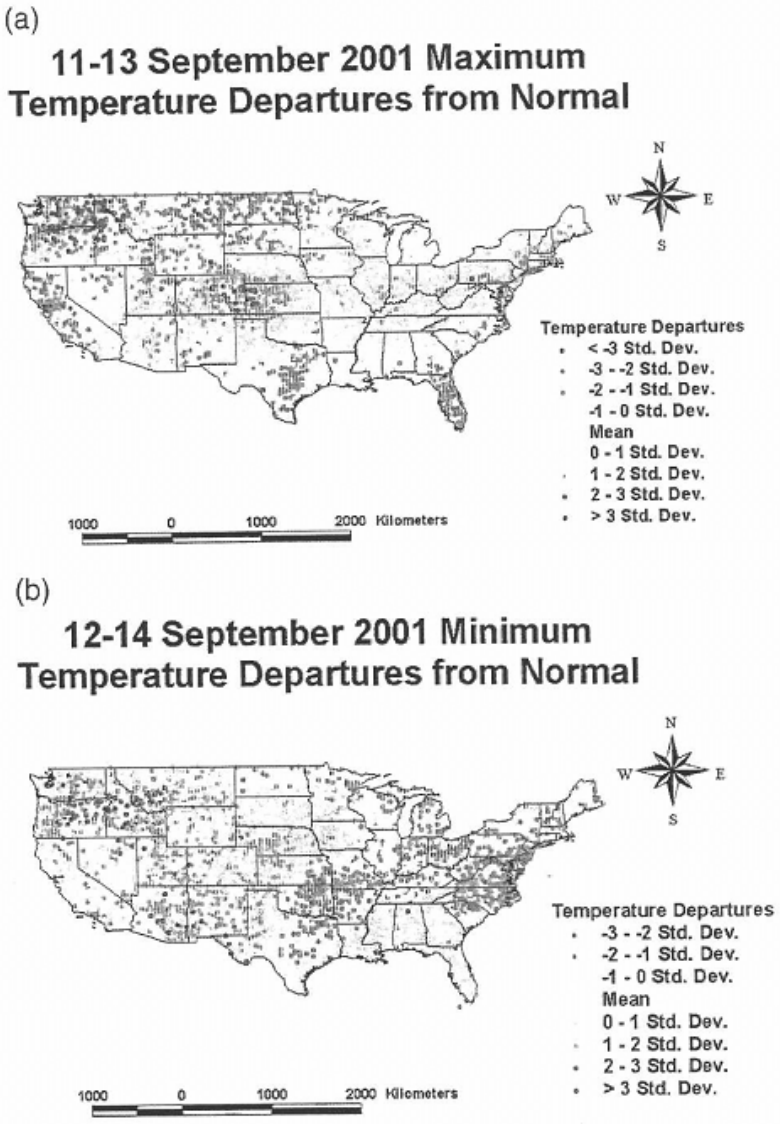


FIG. 2. Map of weather station std dev departures from normal of (a) 11–13 Sep 2001 max temperature ($T_{max}$), and (b) 12–14 Sep 2001 min temperature ($T_{min}$).

climate record have been based mostly on circumstantial evidence; from comparisons of locations with high frequencies of jet aircraft flights or contrails to adjacent locations having fewer (Changnon 1981; Travis and Changnon 1997; Allard 1997). Accordingly, it has been difficult to quantify a contrail effect because of the lack of a comparison "control" period during which persisting contrails were absent significantly longer than their typical life span. The grounding of all commercial aviation in U.S. airspace for approximately 72 h between 11 and 14 September 2001 that followed the terrorist hijackings of four jetliners in U.S. airspace pro-

VI, 6



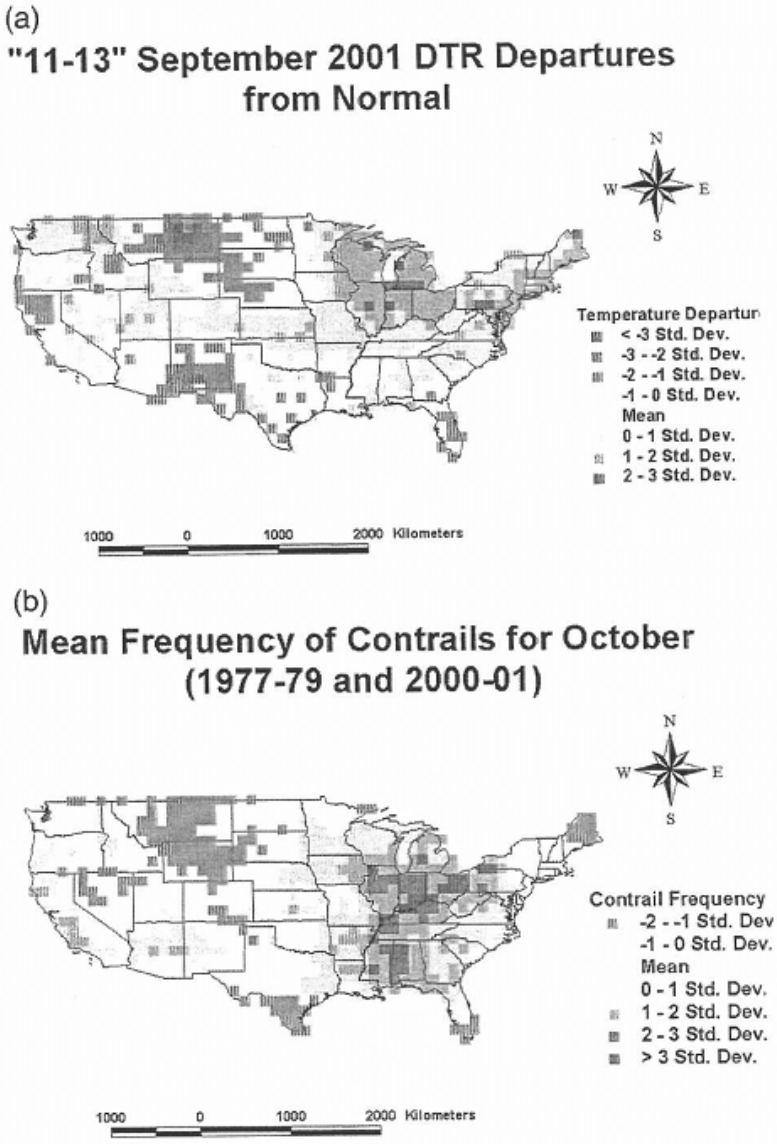


FIG. 3. Map of 1° × 1° resolution (a) grid cell–averaged DTR std dev departure values from long-term (1971–2000) normals for 11–13 Sep 2001, and (b) the combined 1977–79 and 2000–01 mean contrail frequency for Oct.

vides an unexpected opportunity to investigate the regional-scale as well as U.S.-wide effects of contrails on DTR. Our previous study (Travis et al. 2002) has shown that the U.S.-averaged DTR departure for the grounding period increased by approximately 1°C compared to the long-term normals (1971–2000), and 1.8°C compared to the average departure of the adjacent 3-day periods.

To evaluate the presence and magnitude of U.S. re-

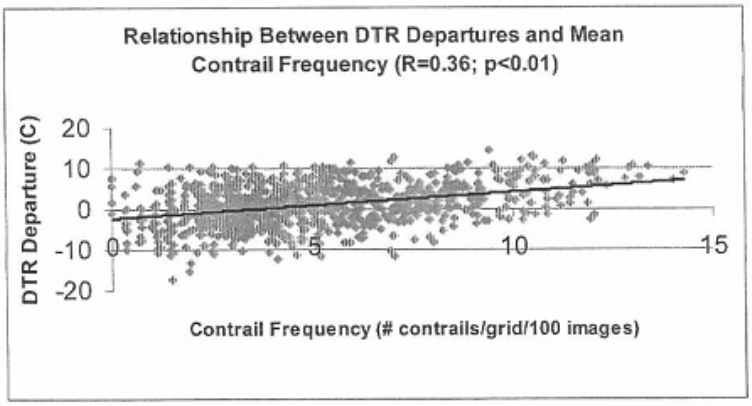


FIG. 4. Scatterplot of the relationship between 11–13 Sep 2001 DTR departures and mean combined 1977–79 and 2000–01 contrail frequency for Oct ($R = 0.36$; $p < 0.01$).

gional-scale DTR anomalies during the grounding period, and determine any associations with the frequency of contrail coverage typically experienced during the fall season, we utilize combinations of surface temperature observations, high-resolution satellite data, and synoptic-scale meteorological reanalyses. Moreover, we provide evidence linking the lack of jet contrails during the grounding period to most observed increases in regional DTR, and also to the asymmetric changes in maximum and minimum temperatures from which DTR is derived.

## 2. Data and methods

### *a. Station temperature data*

Station data on the daily maximum temperature ($T_{max}$) and minimum temperature ($T_{min}$) for all first-order, automated, and cooperative stations in the United States, were obtained from the National Climate Data Center (NCDC 2003) for the most recent 30-yr "normals" period (1971–2000), plus 2001 for the grounding period. Although daily normals were available for a total of 5556 stations, data for only 5404 of those stations were available for the 2001 study period. In addition, many of the stations were cooperative observing sites that record maximum and minimum temperatures from only one observation per 24-h period, unlike the remaining first- and second-order stations that compute daily maxima and minima from continuous observations starting after midnight each day. Thus, it was necessary to standardize the cooperative data by observing time. To ensure that the daily maxima and minima for 11–14 September 2001 were assigned to the correct day, we only included those stations that recorded observations between 0700–0900 or after 1600 local time (LT). When observations were recorded between 0700 and 0900 LT the $T_{max}$ value was assumed to represent the value for the previous day, and when observed after 1600 LT, for the current day. Because only observations from 0700 LT and later were included, each daily $T_{min}$ was assumed to represent the current day's value. These standardization efforts still allowed 4233 stations to be utilized in the temperature analyses, with a reasonably even distribution across the United States (Fig. 2).

Because the aircraft-grounding period began during midmorning (eastern standard time) on 11 September and ended around noon on 14 September,[1] it was necessary to stagger the calculations of average $T_{max}$, $T_{min}$, and DTR across adjacent days. Thus, the afternoon of 11 September and the morning of 14 September represent the beginning and end periods, respectively, of the analysis. The average $T_{max}$ was calculated as the mean of all such observations for 11–13 September (Fig. 2a) and the mean $T_{min}$ was calculated as the average of all such observations for 12–14 September (Fig. 2b). The DTR values for "11 September" were calculated by subtracting each station's minimum temperature on 12 September from its maximum on 11 September, and similarly for the rest of the grounding period. The DTR values so calculated were then averaged for the "11–13" September 2001 period. To evaluate DTR values for the 3-day grounding period in context of the contemporary climatology, we calculated DTR in a similar way for each 11–13 September period for 1971–2000; thus, providing long-term station DTR normals (NCDC 2003). DTR departures for 11–13 September 2001 were then calculated by subtracting station values for 2001 from the corresponding 1971–2000 normals.

[1] A relatively small number of short flights (approximately 4000) took place during the evening of 13 September to reposition aircraft that were redirected during the shutdown on the morning of 11 September. These should not affect the conclusions of this study.

VI, 8



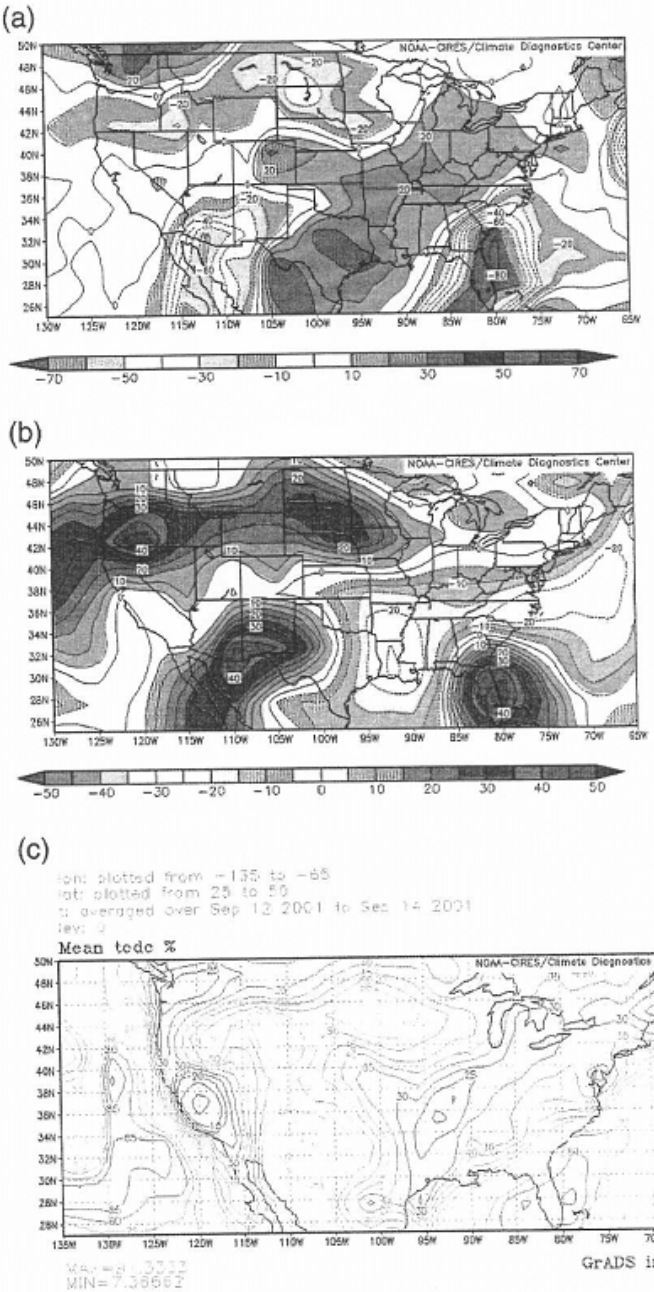


FIG. 5. Mapped 3-day average (12–14 Sep 2001) of (a) anomalies of OLR in W m$^{-2}$, (b) anomalies of relative humidity at 500 hPa; RH(500) in percent; and (c) mean percentage of total cloud sky coverage, derived using the NCEP–NCAR reanalyses.

*b. Satellite data on contrail outbreaks*

To best represent the variations in frequency and density of "typical" contrail coverage across the United States during the fall season for both the recent historical and contemporary periods, we combined two satellite-based data sources of contrail frequency: one previously published and the other original. The first was an analysis of contrail frequency over the conterminous United States for the 1977–79 period based on manual interpretation of high-resolution (0.6 km) Defense Meteorological Satellite Program (DMSP) satellite imagery (DeGrand et al. 2000). This study determined the frequency of contrail occurrence per 1° × 1° grid cells for each of the four midseason months. October was the closest month to our study period and provides an approximation of contrail frequency for the fall season (DeGrand et al. 2000). The procedures used in the recent historical contrail study were duplicated here for the months of October 2000 and 2001, to estimate contrail frequency for the contemporary fall season period. The only exception to this was the satellite data source. For 2000–01, the nonavailability of a dataset having identical temporal and spatial resolutions to the DMSP imagery necessitated that we use data from the Advanced Very High Resolution Radiometer (AVHRR). The AVHRR has a slightly coarser nadir resolution (1.1 km) yet comparable temporal and spatial coverage to that of the DSMP for the 1977–79 period. The slight decrease in resolution of the AVHRR compared with the DMSP should have only a small impact on the ability to recognize *single* contrails (Detwiler and Pratt 1984). More importantly, from the climatic perspective, our use of AVHRR should not substantially impact the relative frequency of regional contrail coverage (i.e., that due to multiple contrails occurring simultaneously). An average of four images per day were analyzed across the two study periods to approximate the regional variations in mean contrail frequency during the climate normals and 2001 periods. The locations of each contrail were stored in a geographic information system (GIS) database [Environmental Systems Research Inc., (ESRI) 1999] for subsequent manipulation and statistical analyses.

Contrails are best distinguished from natural clouds using the infrared band 4 of the AVHRR that is present on all of the National Oceanic and Atmospheric Administration (NOAA) polar-orbiting satellites. We followed the manual pattern recognition method described in Carleton and Lamb (1986) and DeGrand et al. (2000). This method identifies contrails as linear cloud features that are oriented in random directions, unlike natural high clouds, which typically follow the prevailing synoptic flow of the upper troposphere (e.g., Fig. 1). We obtained the contrail dataset for the recent historical period and combined it with our contemporary data to produce mean 1° × 1° resolution contrail frequencies for the conterminous United States.

To permit statistical analyses comparing DTR departures with these satellite-based contrail data it was also necessary to convert all of the point-location weather station observations into grid-averaged (1° × 1°) values. This was accomplished using the same contrail grid GIS database, and spatially associating the location of each grid cell with the underlying weather stations. We then calculated the average temperature values for all weather stations within each cell. The U.S.-averaged number of stations per grid cell was 3.2. When no weather stations existed in a particular grid cell (for 26 of 900 total grids) the grid value was interpolated from the four adjacent grid values. If four adjacent grid values were not available (e.g., along international border and coastal regions) the grid was not included in any further analysis. This procedure resulted in a total of 882 grid cells (98%), containing both fall season contrail frequencies and 11–13 September DTR anomalies, to test the hypothesis that an association existed between the two.

*c. Analysis of synoptic weather conditions*

To more definitively link the regional DTR anomalies with the absence of jet contrails during the grounding period, it is necessary to evaluate the synoptic weather conditions occurring over the conterminous United States. For example, a stagnant weather pattern with anomalously dry air (i.e., low humidity, lack of optically thick clouds) over a large region of the United States for the greater part of the 3-day period, could provide an alternative explanation for the observed anomalous increases in U.S.-averaged DTR (Travis et al. 2002). We used the National Centers for Environmental Prediction–National Center for Atmospheric Research (NCEP–NCAR) reanalysis daily-averaged data on top-of-the-atmosphere outgoing longwave radiation (OLR) as a surrogate for cloud cover, and 500-hPa relative humidity to depict tropospheric moisture for the grounding period [NOAA–CIRES (Cooperative Institute for Research in Environmental Sciences) 2002]. We computed the 3-day-averaged departure of each parameter for the grounding period (12–14 September) from its corresponding climatological normal. These were compared to the maps of DTR and $T_{max}$ and $T_{min}$ for the same period for visual associations.

*d. Application of a contrail outbreak "retro-prediction" method*

It is instructive to estimate where contrails likely would have occurred if commercial aircraft flights had continued as normal for the 11–13 September period. For this purpose we developed a "retro-prediction" (retrodiction) statistical method for contrail outbreaks occurring in otherwise clear air. The retrodiction method uses statistical composites (i.e., ensemble averages and variances) of the upper-tropospheric (300, 250, 200 hPa)

meteorological conditions associated with 48 outbreaks that occurred over the conterminous United States during the 8–16 September periods of 1995–97 and 1999–2001 (the calibration period). Data on meteorological parameters (temperature, humidity, vertical wind shear, vertical motion) previously shown (e.g., Appleman 1953; Schrader 1997; Travis 1996; Travis et al. 1997; Chlond 1998; Kästner et al. 1999) to influence the formation likelihood and persistence time of contrails, were acquired for each outbreak using the 6-hourly NCEP–NCAR reanalyses (Kistler et al. 2001). The outbreak data were then expressed as anomalies from the long-term means for each variable, pressure level, and location, and averaged to yield the composites. For the calibration period, the following outbreak meteorological variables/tropospheric levels were statistically different from climatology: increased values of humidity at 300 hPa (RH range = +7.5%–+58.0%), lower temperature and reduced $Z_{300}$–$Z_{200}$ thickness (−6.5 m), light easterly $u$-wind anomalies at 250 hPa (range = −2.2 to −2.9 m s$^{-1}$), and slightly negative (i.e., upward) vertical motion (mean = $-0.54 \times 10^{-3}$ Pa s$^{-1}$ at 250 hPa). Using GIS, we applied the outbreak composite statistical ranges to two independent sets of reanalyses "test" periods: 8–16 September 1998, and the day immediately preceding, and also immediately following the grounding period. The AVHRR imagery for these periods was also inspected for contrail outbreaks. Using a test criterion of a minimum of 50% spatial overlap between the retrodicted and observed contrail outbreaks, we found good agreement (25 out of the 30 cases). This allowed us confidently to apply the method to the upper-tropospheric reanalyses for the grounding period. The resulting contrail-favored areas (CFAs) mapped locations, and their associations with DTR departures, are discussed in section 3d.

## 3. Results and discussion

### a. $T_{max}$ and $T_{min}$ spatial trends

Although both the 3-day U.S.-averaged $T_{max}$ and $T_{min}$ were warmer than normal for the grounding period, the $T_{min}$ increase (0.3°C) was about one-fourth that of $T_{max}$ (1.2°C). This asymmetric variation from the long-term means may indicate that the lack of contrails impacted the daytime temperatures more than those at night. Such a possibility accords with the observed greater frequencies of contrails during daytime versus nighttime hours, in association with diurnal differences in the frequencies of jet aircraft flights (Bakan et al. 1994; Minnis et al. 1997).

The spatial patterns of $T_{max}$ for 11–13 September 2001 (Fig. 2a) show strongest increases in the Intermountain West and Pacific Northwest, extending through the Midwest and into the northeast United States. Strongest decreases of $T_{max}$ occurred in California, the northern Great Plains, the Southwest, and Florida. For $T_{min}$ (Fig. 2b) the largest increases were in the West (except California) and the Gulf Coast states. The largest combined increase of $T_{max}$ and $T_{min}$ occurred in portions of the Northwest. This can be partially attributed to a persistent southerly flow that was produced from synoptic-scale circulations associated with a storm system centered off the northern California coast for much of the grounding period. This storm also likely contributed to the large decrease in $T_{max}$ seen in northern California due to extensive daytime cloud coverage. Strong decreases in $T_{min}$ occurred through the southern Great Plains, Midwest and Great Lakes, the Mid-Atlantic region, and the northeast United States. Possible associations between these spatial variations of $T_{max}$ and $T_{min}$ departures, and the lack of contrails during the grounding period, are discussed in section 3c.

### b. DTR spatial trends and associations with contrail frequency

The spatial variation of the grid-averaged DTR anomalies for the grounding period (Fig. 3a) shows that the largest positive departures extended across portions of the central and northeast United States as well as the Pacific Northwest. Because these regions have previously been reported (Minnis et al. 1997; DeGrand et al. 2000) as being climatologically favorable for outbreaks of persisting contrails, we argue that this anomalous increase was associated with the absence of contrails during the aircraft groundings (Travis et al. 2002), in combination with synoptic conditions.

To identify the relationship between the regional DTR increases of the grounding period and spatial variations in the typical fall-season contrail coverage, Fig. 3b summarizes the mean contrail frequency (combined 1977–79, 2000–01) averaged for the same 1° × 1° grids as the DTR data. The frequency pattern of contrails for this period appears broadly similar to that shown in previous studies for other times of the year (Minnis et al. 1997; DeGrand et al. 2000), with the contrail frequency maxima occurring in the Midwest, Southeast, and parts of the West.

Visual comparison of Figs. 3a and 3b suggests some agreement between those regions having the largest increases in DTR during the grounding period and those typically experiencing the greatest contrail coverage during the fall season. To quantify the presence and strength of this relationship a Pearson correlation coefficient was calculated between DTR departure and contrail frequency for the 882 grids available for analysis (Fig. 4). The statistically significant positive relationship ($R = 0.36$; $p < 0.01$) supports our contention that a contrail-induced suppression of DTR was present in the 1971–2000 normals throughout much of the United States, and especially in areas where contrails are typically most prevalent. Moreover, the gradual reduction in statistical scatter about the trend line as contrail frequency increases may indicate that the contrail "sig-

nal" in DTR departure was more distinguishable from synoptic-scale "background" influences for those grids having the highest mean contrail frequency.

### c. Synoptic variations in cloud and humidity during the grounding period

The 3-day average (12–14 September 2001) OLR anomaly map (Fig. 5a) shows positive departures (i.e., fewer clouds or lower mean cloud-top altitude) in a swath extending from the south-central United States through the Midwest and into the mid-Atlantic regions. A smaller area of OLR positive departures also occurred in the Pacific Northwest. In contrast, OLR negative departures (i.e., more clouds or higher mean cloud-top altitude) occurred over the Southwest, Florida, and the extreme southeast United States, and parts of the Intermountain West extending through the northern Great Plains. The remainder of the country had close to normal departures of OLR for the grounding period. A comparison of the OLR anomaly field with that of the midtropospheric (500 hPa) relative humidity [RH(500); Fig. 5b], shows general consistency: areas of positive (negative) relative humidity departure accompany increased moisture and ascent of air (decreased moisture and subsidence), and tend to be associated with negative (positive) anomalies of OLR (Fig. 5a). Thus, about one-half of the United States experienced fewer or lower-altitude clouds than normal during the grounding period; the other half had either near-normal or more than normal/deeper clouds. This statement is supported by the analysis of the mean percentage of total cloud coverage (TCDC; departures not available) for the grounding period (Fig. 5c), which shows good agreement with the OLR departures in most areas of the United States. Stratifying the 3-day averaged RH(500) into daytime and nighttime components (Fig. 6) also shows strong spatial consistency and reduces the possibility that the asymmetrical departures of $T_{max}$ and $T_{min}$ reported in section 3a are a result of large diurnal variations in relative humidity.

It is particularly interesting that some of the largest DTR and $T_{max}$ anomalies in the Intermountain West occurred near the outer edges of the areas having the most positive anomalies of humidity and deepest cloud cover (i.e., Colorado, Utah; Fig. 5). The lack of clouds in the adjacent areas suggests that although moisture levels were above normal (Fig. 5b), they were not sufficient for substantial cloud coverage to form through natural processes. However, because such environments are often conducive to contrail formation [i.e., high humidity but few clouds; Travis et al. (1997); section 3d], it is reasonable to assume that contrails likely would have formed in these areas had airplanes been flying. This implies that the lack of contrails in those areas helped offset the tendency for DTR to decrease when averaged over the 3-day grounding period. Such a possibility is now evaluated using the CFA retrodictions for the same period.

### d. Retrodicted contrail outbreaks and associations with DTR anomalies

Figure 7 depicts the grounding-period CFAs derived from the contrail-outbreak retrodiction method (section 2d). To facilitate visual comparisons with the DTR departure map (Fig. 3a), the CFAs were converted to $1° \times 1°$ grids for locations where contrail occurrence was favorable for a minimum of at least 12 h during the grounding period ("moderate susceptibility"). Grid cells over which CFAs existed for more than 50% of the grounding period (i.e., 36 h) were deemed to have "high susceptibility." All remaining grid cells were designated as having "low susceptibility" (Fig. 7). The Pacific Northwest, Intermountain West, and Southwest U.S. regions were highly susceptible to contrails during the grounding period (Fig. 7). Smaller regions of contrail high susceptibility included the Midwest, Great Lakes, and Florida. These high susceptibility CFAs coincide with the edges of the positive moisture anomaly areas (Fig. 5b). Such a result concurs well with previous research on contrail–synoptic weather associations, which has reported that contrails occur most commonly along the leading edge of cirrus shields associated with frontal cyclones and convective storms (Detwiler and Pratt 1984; Travis et al. 1997; DeGrand et al. 2000).

A visual comparison of the departure maps for $T_{max}$ and $T_{min}$ (Figs. 2a,b) with Figs. 5 and 7 suggests that $T_{max}$ shows a closer association with the CFA high susceptibility retrodiction (except for Florida), whereas $T_{min}$ shows a closer association with the synoptics; specifically, OLR and total cloud cover. This may imply that the lack of contrails affected $T_{max}$ more than $T_{min}$ during the grounding period, especially in the West. There, the combination of a warm, moist southerly flow and the lack of airplanes led to increasing humidity and temperature but less cloud coverage than otherwise would have occurred from contrail formation; especially during the daytime when air traffic would normally have been greatest (with less impact on $T_{max}$). In the eastern half of the United States, the increased DTR seems to have resulted from a combination of dry air and lack of clouds (lowers $T_{min}$, raises $T_{max}$ and DTR) and the lack of contrails. This is consistent with the observation (section 3a) that the U.S.-averaged $T_{max}$ increased more than $T_{min}$ during the grounding period.

Comparing Fig. 7 with the DTR departure map (Fig. 3a) shows strong agreement for much of the west, especially in the Intermountain and Northwest regions. For the entire conterminous United States the average DTR departure for the high susceptibility grid cells (+1.3°C) is statistically greater ($p < 0.01$) than that for the moderate susceptibility (+0.9°C) and the low susceptibility grid cells (+0.8°C). The slightly higher av-

VI, 12



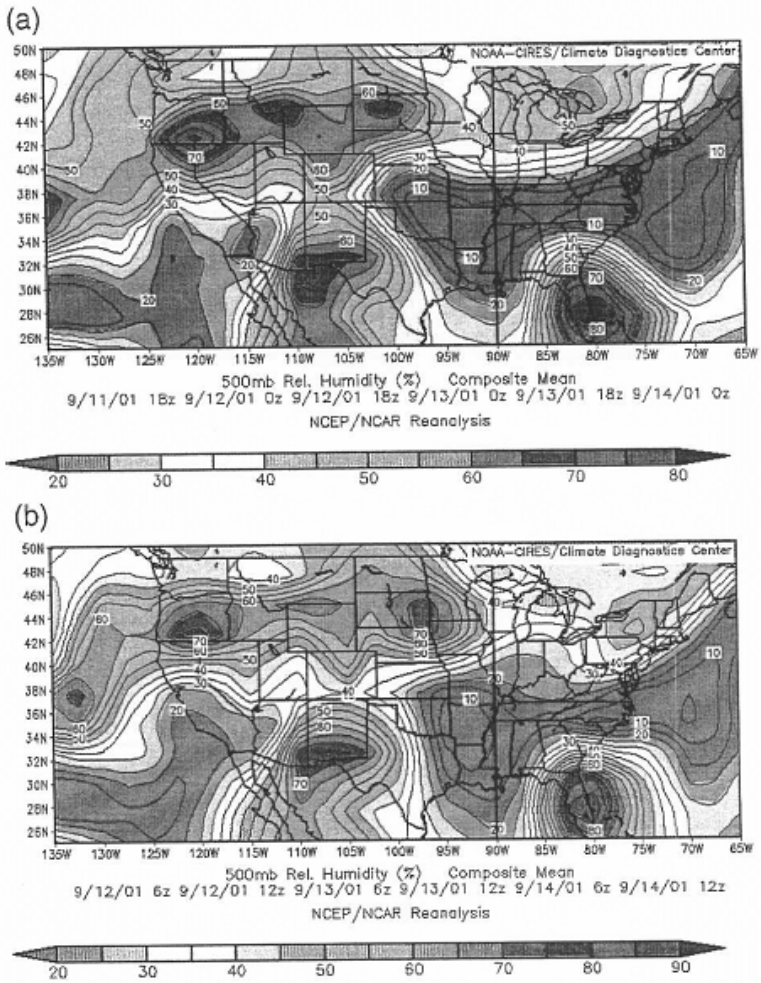


FIG. 6. Mapped 3-day average (1800 UTC 11 Sep 2001–1800 UTC 14 Sep 2001) anomalies of relative humidity at 500 hPa: RH(500) in percent for (a) daytime periods (0000 and 1800 UTC) and (b) nighttime periods (0600 and 1200 UTC), derived using the NCEP–NCAR reanalysis.

erage DTR departures in the moderate susceptibility grid cells compared with the low susceptibility cells are not statistically different. These results further support our contention that the lack of commercial aircraft flying, especially in the areas of contrail high susceptibility, contributed to the 11–13 September DTR anomaly. In combination with the statistical relationship shown earlier between DTR departure and the fall-season contrail frequency (section 3b), this finding implies that the 11–13 September DTR anomaly was caused by a combination of regional-scale, contrail-induced suppression of DTR in the long-term climatological normals and the presence of extensive areas of contrail high susceptibility, which remained unexploited owing to the lack of commercial aircraft flights.

## 4. Summary and conclusions

These results support the hypothesis that the grounding of all commercial aircraft in U.S. airspace, and the consequent elimination of substantial jet contrail coverage during the 11–14 September 2001 grounding pe-

VI, 13



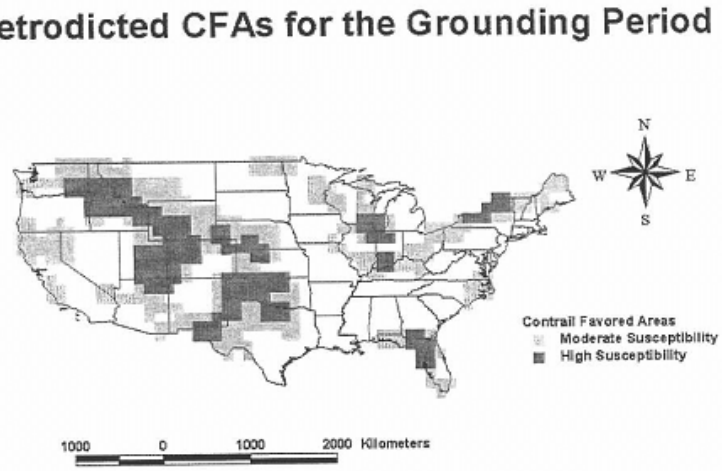


FIG. 7. Grid cell-averaged (1° × 1° resolution) map of CFAs determined for the grounding period (1800 UTC 11 Sep 2001–1800 UTC 14 Sep 2001) using the contrail-outbreak retrodiction method applied to the six-hourly NCEP–NCAR reanalyses of the upper troposphere (refer to text). The lighter (darker) shading refers to moderate (highest) susceptibility of contrail outbreaks. Those regions that were not susceptible to outbreaks are not shaded.

riod, helped produce an enhanced surface DTR in those areas that typically experience the greatest numbers of jet contrails during the fall season (e.g. the Midwest). The DTR anomaly occurred primarily due to large increases in $T_{max}$ that were not matched by similar magnitude increases in $T_{min}$. In the West, synoptic weather patterns (mostly cyclonic) during the grounding period appear to have played an important role in enhancing (e.g., the Intermountain region) or negating (e.g., coastal California) the effect of contrail absence on surface temperature. For the country as a whole, the synoptic weather conditions during the grounding period suggest a better association of these with $T_{min}$ than $T_{max}$ thus providing a possible partial explanation for the asymmetric response of these two components of DTR.

Our analyses of the AVHRR imagery available for the grounding period indicated several occurrences of single contrails (no outbreaks) produced by military aircraft, including some in the Northeast that demonstrated extensive persistence and spreading characteristics (Minnis et al. 2002). Moreover, the analysis of other imagery showed many contrails occurring just over the border in Canada. When combined with the statistical model retrodictions, these observations suggest that if commercial airplanes had not been grounded, substantial contrail coverage would have been present over large parts of the United States, especially the Pacific Northwest, Intermountain West, upper Midwest, and Great Lakes and the Northeast.

Predicted future increases in aircraft flight frequencies, and subsequent increased occurrences of contrails in the climatologically susceptible extratropics (e.g., Gierens et al. 1999; Minnis et al. 1999), could lead to an even greater influence on DTR. However, potential changes in upper-tropospheric conditions related to global-scale climate change, which can influence both the formation likelihood and persistence time of contrails, need to be considered when projecting future impacts of contrails onto regional-scale climate.

*Acknowledgments.* This research was sponsored by grants from the National Science Foundation (BCS-0099011 and BCS 0099014). We are grateful to the following for their contributions to this research: Mr. Jeff Johnson (University of Wisconsin—Whitewater) for assisting with the 2000–01 contrail satellite analysis; Mr. James Q. DeGrand (The Ohio State University) for providing the 1977–79 satellite contrail frequency dataset; and the two anonymous reviewers, for their many helpful and insightful comments.

## REFERENCES

Allard, J., 1997: The climatic impacts of jet airplane condensation trails (contrails) in the Northeast U.S. M.S. thesis, Dept. of Geography, The Pennsylvania State University, 152 pp. [Available from Dept. of Geography, The Pennsylvania State University, University Park, PA 16802.]

Appleman, H., 1953: The formation of exhaust condensation trails by jet aircraft. *Bull. Amer. Meteor. Soc.*, **34**, 14–20.

Bakan, S., M. Betancor, V. Gayler, and H. Grassl, 1994: Contrail frequency over Europe from NOAA-satellite images. *Ann. Geophys.*, **12**, 962–968.

Carleton, A. M., and P. J. Lamb, 1986: Jet contrails and cirrus cloud: A feasibility study employing high-resolution satellite imagery. *Bull. Amer. Meteor. Soc.*, **67**, 301–309.

VI, 14



Changnon, S. A., 1981: Midwestern cloud, sunshine and temperature records since 1901: Possible evidence of jet contrail effects. *J. Appl. Meteor.*, **20,** 496–508.

Chlond, A., 1998: Large-eddy simulations of contrails. *J. Atmos. Sci.*, **55,** 796–819.

DeGrand, J. Q., A. M. Carleton, D. J. Travis, and P. Lamb, 2000: A satellite-based climatic description of jet aircraft contrails and associations with atmospheric conditions, 1977–79. *J. Appl. Meteor.*, **39,** 1434–1459.

Detwiler, A., and R. Pratt, 1984: Clear-air seeding: Opportunities and strategies. *J. Wea. Modif.*, **16,** 46–60.

Duda, D. P., P. Minnis, and L. Nguyen, 2001: Estimates of cloud radiative forcing in contrail clusters using GOES imagery. *J. Geophys. Res.*, **106,** 4927–4937.

ESRI, 1999: ArcView 3.2. Environmental Systems Research Inc.

Gierens, K., R. Sausen, and U. Schumann, 1999: A diagnostic study of the global distribution of contrails. Part II: Future air traffic scenarios. *Theor. Appl. Climatol.*, **63,** 1–9.

Gothe, M. B., and H. Grassl, 1993: Satellite remote sensing of the optical depth and mean crystal size of thin cirrus and contrails. *Theor. Appl. Climatol.*, **48,** 101–113.

Karl, T. R., and Coauthors, 1993: Asymmetric trends of daily maximum and minimum temperature. *Bull. Amer. Meteor. Soc.*, **74,** 1007–1023.

Kästner, M., R. Meyer, and P. Wendling, 1999: Influence of weather conditions on the distribution of persistent contrails. *Meteor. Appl.*, **6,** 261–271.

Kistler, R., and Coauthors, 2001: The NCEP–NCAR 50-Year Reanalysis: Monthly means CD-Rom and documentation. *Bull. Amer. Meteor. Soc.*, **82,** 247–267.

Meerkotter, R., U. Schumann, D. R. Doelling, P. Minnis, T. Nakajima, and Y. Tsushima, 1999: Radiative forcing by contrails. *Ann. Geophys.*, **17,** 1080–1094.

Mims, F. M., III, and D. J. Travis, 1997: Reduced solar irradiance caused by aircraft contrails. *Eos, Trans. Amer. Geophys. Union*, **78,** 448.

Minnis, P., J. K. Ayers, and S. P. Weaver, 1997: Surface-based observations of contrail occurrence frequency over the U.S., April 1993–April 1994. NASA Ref. Publ. 1404, May 1997, 12 pp. and tables and figs.

——, U. Schumann, D. R. Doelling, K. M. Gierens, and D. W. Fahey, 1999: Global distribution of contrail radiative forcing. *Geophys. Res. Lett.*, **26,** 1853–1856.

——, L. Nguyen, D. P. Duda, and R. Palikonda, 2002: Spreading of isolated contrails during the 2001 air traffic shutdown. Preprints, *10th Conf. on Aviation, Range, and Aerospace Meteorology*, Portland, OR, Amer. Meteor. Soc., 33–36.

Murcray, W. B., 1970: On the possibility of weather modification by aircraft contrails. *Mon. Wea. Rev.*, **98,** 745–748.

NCDC, 2003: Data documentation for Data Set 3200 (DSI-3200). National Climatic Data Center Tech. Doc. 3200, Asheville, NC, 18 pp. [Available online at ftp://ftp.ncdc.noaa.gov/pub/data/documentlibrary/tddoc/td3200.doc.]

NOAA–CIRES, cited 2002: Online Reanalysis Data. NOAA–CIRES Climate Diagnostics Center, Boulder, CO. [Available online at www.cd.noaa.gov.]

Penner, J. E., D. H. Lister, D. J. Griggs, D. J. Dokken, and M. McFarland, Eds., 1999: Aviation and the Global Atmosphere. Intergovernmental Panel on Climate Change, 12 pp.

Sassen, K., 1997: Contrail-cirrus and their potential for regional climate change. *Bull. Amer. Meteor. Soc.*, **78,** 1885–1903.

Schrader, M. L., 1997: Calculations of aircraft contrail formation critical temperatures. *J. Appl. Meteor.*, **36,** 1725–1728.

Travis, D. J., 1996: Variations in contrail morphology and relationships to atmospheric conditions. *J. Wea. Modif.*, **28,** 50–58.

——, and S. A. Changnon, 1997: Evidence of jet contrail influences on regional-scale diurnal temperature range. *J. Wea. Modif.*, **29,** 74–83.

——, ——, and S. A. Changnon, 1997: An empirical model to predict widespread occurrences of contrails. *J. Appl. Meteor.*, **36,** 1211–1220.

——, ——, and R. Lauritsen, 2002: Contrails reduce daily temperature range. *Nature*, **418,** 601.

VI, 15



KING'S College LONDON



About
Search news archive
Public Relations
Add an event

# News highlights

Print version

## Proof that airports are air polluters

22 Apr 2010, PR 89/10

**Scientists in the Environmental Research Group (ERG) at King's have undertaken research into the effects of the closure of UK airspace on air quality surrounding major airports after the Icelandic volcano eruption, following a number of enquiries from the public.**

In response the ERG analysed the concentrations of NOX (the generic term for oxides of nitrogen combined) and NO2 (nitrogen dioxide) surrounding Gatwick and Heathrow airports during the first three days of closure, Thursday 15 to Saturday 17 April 2010. This period was chosen due to the stable weather conditions with light north easterly winds, allowing a cross-sectional analysis upwind and downwind of the airports.

This period of unprecedented closure during good weather conditions allowed the scientists to demonstrate that the airports have a clear measurable effect on nitrogen concentrations and that this effect disappeared entirely during the period of closure.

**Pollution impact**

Such nitrogen pollutants can increase breathing difficulties in people with existing sensibilities, cardiac conditions or in older people. Under the impact of sunlight they can transform into the even more damaging pollutant ozone. NOx and NO2 are particularly associated with jet aircraft, as they are produced by the high-temperature mix of aviation with fuel.

The analysis was undertaken by Dr Ben Barratt and Dr Gary Fuller of the Environmental Research Group, School of Biomedical and Health Sciences. *'We have always been fairly confident that there was this 'airport effect' but we have never been able to show it,'* said Dr Barratt. *'The closure gave us the opportunity to look at it, and there is a very strong indication that it is the case.*

*'This exceptional closure has allowed us to demonstrate the impacts of airport emissions on their immediate neighbourhood. We did not consider the impact of decreased traffic flows on airport feeder roads in this preliminary study. Decreased traffic flows are likely to have a significant effect on concentrations of vehicle-related pollutants close to such roads, but unfortunately*

News by year
- News highlights
- News archive 2009
- News archive 2008
- News archive 2007
- News archive 2006
- News archive 2005
- News archive 2004
- News archive 2003
- News archive 2002
- News archive 2001
- News feed

VI, 16

*we did not have sufficient traffic data to carry out this analysis at that time,' he continued.*

A full version of the report is available for download from the ERG's *London Air Quality Network* website.

**Notes to editors**

**King's College London**
King's College London is one of the top 25 universities in the world (*Times Higher Education* 2009) and the fourth oldest in England. A research-led university based in the heart of London, King's has nearly 23,000 students (of whom more than 8,600 are graduate students) from nearly 140 countries, and some 5,500 employees. King's is in the second phase of a £1 billion redevelopment programme which is transforming its estate.

King's has an outstanding reputation for providing world-class teaching and cutting-edge research. In the 2008 Research Assessment Exercise for British universities, 23 departments were ranked in the top quartile of British universities; over half of our academic staff work in departments that are in the top 10 per cent in the UK in their field and can thus be classed as world leading. The College is in the top seven UK universities for research earnings and has an overall annual income of nearly £450 million.

King's has a particularly distinguished reputation in the humanities, law, the sciences (including a wide range of health areas such as psychiatry, medicine and dentistry) and social sciences including international affairs. It has played a major role in many of the advances that have shaped modern life, such as the discovery of the structure of DNA and research that led to the development of radio, television, mobile phones and radar. It is the largest centre for the education of healthcare professionals in Europe; no university has more Medical Research Council Centres.

King's College London and Guy's and St Thomas', King's College Hospital and South London and Maudsley NHS Foundation Trusts are part of King's Health Partners. King's Health Partners Academic Health Sciences Centre (AHSC) is a pioneering global collaboration between one of the world's leading research-led universities and three of London's most successful NHS Foundation Trusts, including leading teaching hospitals and comprehensive mental health services. For more information, visit: www.kingshealthpartners.org.

**Further information**
Kate Moore
Public Relations Officer (Health Schools)
Email: kate.moore@kcl.ac.uk
Tel: 020 7848 4334

Next:
Who is watching you?
More Swedes than Brits survive lung cancer
Edmund-Davies Professor of Criminal Law appointed
Santander's chairman visits King's
Leading academic warns of 'care squeeze' in NHS

VII, C

# APPENDIX 7

VII, 2





Email / Share Back One



# Does Air Pollution Increase Rainfall

Posted in | Energy | Climate Change | Global Warming | Pollution | Water



**An international team of scientists, headed by Prof. Daniel Rosenfeld of the Institute of Earth Sciences at the Hebrew University of Jerusalem, has come up with a surprising finding to the disputed issue of whether air pollution increases or decreases rainfall. The conclusion: both can be true, depending on local environmental conditions.**

The determination of this issue is one with significant consequences in an era of

VII, 3




- Popular
- Latest
- Random

Morgan Solar Raises $8.2 Million for Concentrated Photovoltaic Solar Panel Development

Evergreen Solar's String Ribbon Panels to power Patriot Place

SunRun Announces Low-Cost Solar Power for Homes in New Jersey

Four Winds Renewable Energy Offers Grid-Tie Solar Electric Systems

Puget Sound Energy Customers Connect Solar Systems to Utility Grid

UD5 and UJ6 PV Modules from Mitsubishi Electric Ready for Installation Near Salt Water

Energy Conversion Devices and Enfinity Corporation to Develop Rooftop Solar Installations in Ontario, Canada

Umwelt-Sonne-Energie Completes Largest Solyndra Rooftop PV System Project in Belgium

A-Power Energy Generation Systems Delivers Wind Turbines in China

Canadian Solar Enters into PV Modules Sales Contract with Fire Energy Group

Northside Lofts Geothermal Project by Middleton Geothermal Services

Energy Conversion Devices and Enfinity Corporation to


climate change and specifically in areas suffering from manmade pollution and water shortages, including Israel.

In an article appearing in the Sept 5 issue of the journal Science, the scientific team, which included researchers from Germany, has published the results of its research untangling the contradictions surrounding the conundrum. They do this by following the energy flow through the atmosphere and the ways it is influenced by aerosol (airborne) particles. This allows the development of more exact predictions of how air pollution affects weather, water resources and future climates.

Mankind releases huge amounts of particles into the air that are so tiny that they float. Before being influenced by man, air above land contained up to twice as many of these so called aerosol particles as air above oceans.

VII, 4

and Enmax Corporation to Develop Rooftop Solar Installations in Ontario, Canada

Research Aims to Reduce Energy Usage in the Home

eSolar and Penglai Electric Announce Licensing Agreement to Build Solar Thermal Power Plants in China

Northern Power Systems Selects Analog Devices' SHARC Processors for its Northwind 100 Community-Scale Wind Turbines

Smoke from agricultural fires suppresses rainfall from a cloud over the Amazon (right). A similar size cloud (left) rains heavily on the same day some distance away in the pristine air. (Hebrew University photo)

Nowadays, this ratio has increased to as much as a hundredfold.

Natural and manmade aerosols influence our climate – that much is agreed. But which way do they push it? They produce more clouds and more rain, some say. They produce fewer clouds and less rain, say others. This disputed role of aerosols has been the greatest source of uncertainties in our understanding of the climate system, including the question of global warming.

"Both camps are right", says Prof. Meinrat O. Andreae, director of the Max Planck Institute for Chemistry in Germany, a coauthor of the publication. "But you have to consider how many aerosol particles there are." The lead author, Prof. Rosenfeld of the Hebrew University, adds: "The amount of aerosols is the critical factor controlling how the energy is distributed in the atmosphere." Clouds, and therefore precipitation, come about when moist, warm air rises from ground level and water condenses or freezes on the aerosols aloft. The energy responsible for evaporating the water from the earth's surface and lifting the air is provided by the sun.

Aerosols act twofold: On the one hand, they act like a sunscreen reducing the amount of sun energy reaching the ground. Accordingly, less water evaporates and the air at ground level stays cooler and drier, with less of a tendency to rise and form clouds.

On the other hand, there would be no cloud droplets without aerosols. Some of them act as gathering points for air humidity, so called condensation nuclei. On these tiny particles with diameters of less than a thousandth of a millimeter the water condenses – similar to dew on cold ground – releasing energy in the process. This is the same energy that was earlier used to evaporate the water from the earth's surface. The

VII, 5

released heat warms the air parcel so that it can rise further, taking the cloud droplets with it. But if there is a surplus of these gathering points, the droplets never reach the critical mass needed to fall to earth as rain – there just is not enough water to share between all the aerosol particles. Also, with a rising number of droplets their overall surface increases, which increases the amount of sunlight reflected back to space and thus cooling and drying the earth.

In a nutshell, then, the study results show the following: With rising pollution, the amount of precipitation at first rises, than maxes out and finally falls off sharply at very high aerosol concentrations. The practical result is that in relatively clean air, adding aerosols up to the amount that releases the maximum of available energy increases precipitation. Beyond that point, increasing the aerosol load even further lessens precipitation. Therefore, in areas with high atmospheric aerosol content, due to natural or manmade conditions, the continuation or even aggravation of those conditions can lead to lower than normal rainfall or even drought.

Prof. Rosenfeld states: "These results have great significance for countries like Israel where rainfall is scarce and can be easily affected by over-production of aerosols. Our study should act as a red light to all of those responsible for controlling the amounts of pollution we release into the atmosphere."

"With these results we can finally improve our understanding of aerosol effects on precipitation and climate," summarizes Andreae, "since the direct contradiction of the different aerosol effects has seriously hindered us from giving more accurate predictions for the future of our climate, and especially for the availability of water."

**Published Date**: 8/9/2008

Click here for Cleantech news archive

Δ Top

VIII

# APPENDIX 8

VIII, 2

**Rain Men: Scientists Here Tried to Change the Weather**

By Chrissie Reilly
Staff Historian

(Note: This article appeared in the 20 Feb 2009 issue of the *Monmouth Message*)

Everybody talks about the weather, but nobody does anything about it.

Except here at Fort Monmouth, where researchers changed the course of nature, and of history, in 1947.

This installation was home to Project Cirrus, a five-year foray into the science, and sometimes the art, of weather modification.

The discoveries and experiments in our very own Signal Corps Laboratories as part of Project Cirrus are still relevant, and the technology is still used worldwide.

The project was led by Nobel laureate Dr. Irving Langmuir and his protégé Dr. Vincent Schaefer, both from General Electric (GE).

Langmuir defined serendipity as "the art of profiting from unexpected occurrences." Their discovery of cloud seeding certainly qualified as one such serendipitous event.

The cloud seeding project originated with experiments in de-icing aircraft that took them to Mount Washington, New Hampshire— home of extremely harsh winter weather.

To recreate these conditions in a lab, Schaefer invented a "cold box" to test his theories. This was a GE home freezer with a black velvet lining and a viewing light.

Employees from Fort Monmouth work on the Project Cirrus equipment.

Breathing into the cold box produced a tiny cloud of supercooled water droplets, just like in the upper parts of a cloud.

Schaefer later discovered that the addition of any substance that was -40 degrees Celsius would cause millions of ice crystals to form in the cloud. They extrapolated that this would work in atmospheric clouds, too.

So the men attempted to 'seed' clouds with dry ice by flying over them and releasing the particles.

VIII, 3

On Nov 13, 1946, Shaefer dropped 1.4 kg of dry ice pellets from an airplane into a supercooled stratus cloud near Schenectady, New York. And snow fell!

In February 1947, the US Army Signal Corps became involved in these cloud seeding missions, and it earned the name Project Cirrus.

The project was a joint effort of the Army, Navy, Air Force, and GE.

William R. Cotton and Roger A. Pielke wrote about Langmuir's and Schaefer's exploration into cloud seeding with cirrus clouds, supercooled stratus clouds, cumulus clouds, and even hurricanes in their book *Human Impacts on Weather and Climate*.

The supercooled stratus clouds were the most responsive to seeding, and patterns (including L-shapes, race tracks, and Greek gammas) could be seeded into the clouds.

Retired Fort Monmouth physicist Sam Stine worked at the Evans Signal Laboratory designing experiments. He then had the job of getting into the airplanes and actually testing them.

According to Stine, "We flew about 37 experimental flights in the first year and a half. Flying into thunderstorms, line squalls, the tops of tornadoes, you have it."

Project Cirrus plane in flight.

Because of the inherent variability in weather patterns, attempts to modify weather did not always yield perfect or consistent results; there was also the problem of reliably attributing results to specific scientific actions.

Dr. Harold Zahl recalled in his book, *Electrons Away, or Tales of a Government Scientist*, "There were conditions when rain or snow could be precipitated, but the moisture had to be there in the first place. Nature had to be a cooperating partner and, when needed most, it seemed that she was not always ready to help."

Cloud seeding did not always produce the expected results.

The first attempt at modifying a tropical cyclone or hurricane occurred in 1947. It was October and a hurricane was head eastward off the coast of Florida and into the Atlantic.

After 80 lbs of dry ice were dispersed into the hurricane, it briefly paused, and then headed for the shore. Winds of 85 mph were clocked in Savannah, GA, a resident there was killed, coastal areas flooded, and the damage totaled over $20 million.

VIII, 4

Jay Barnes and Steve Lyons reported in *Florida's Hurricane History*, that many believed that the seeding was responsible for the turn, including Langmuir. Hurricanes had however behaved like this in the past without seeding – only 40 years prior a hurricane did the same thing and headed due west into the coast.

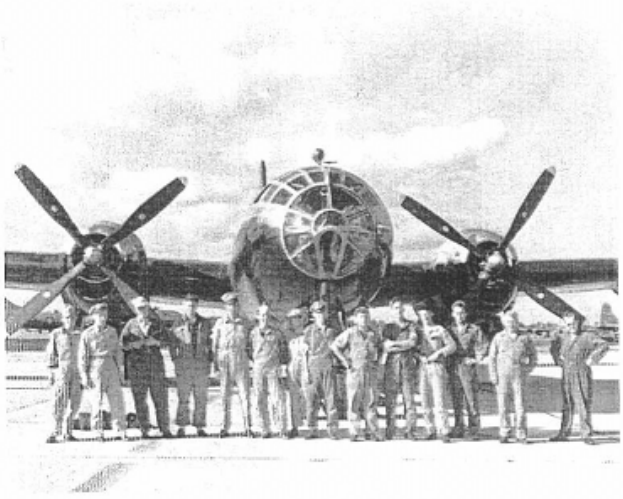

Project Cirrus was a joint effort of the Army, Navy, Air Force, and General Electric. This photo was taken before one of the many flights in 1948.

Zahl reported that "we concluded it was 'an act of God.' If it could happen once, it could happen twice."

Either way, GE's lawyers told Langmuir not to discuss the hurricane until the statute of limitations had run out for prosecution.

The technology involved in Cirrus was put to good use also in October 1947, when clouds were seeded above a Maine forest fire to help extinguish the blaze.

Despite the often mixed results of Project Cirrus, Langmuir was a noted workaholic. *The New York Times* reported that upon his retirement from GE in 1950, he did not even take a vacation, but went straight to devoting more time to Cirrus.

Langmuir told reporters for a March 2, 1950 *New York Times* article that "within the past year, Project Cirrus has grown very greatly in importance, and now I believe that the best service that I can render to the national welfare is to increase my activities in this field."

He also expected the same rigorous work ethic from his lab personnel. On Thanksgiving 1951, he complained that his employees wanted days off for the holiday!

Cloud seeding and weather modification in general declined over the years, due to a number of reasons.

Weather modification was largely oversold to the public and legislative members; an abnormal wet period in the United States reduced demand; and changes in government and public attitudes towards other weather and climate concerns all contributed to less seeding projects over the years.

Despite this controversy, it has not stopped people continuing to try to control the weather.

VIII, 5

The 2008 Olympic Games held in Beijing were scheduled during northern China's rainy season.

In order to prevent rain from ruining the opening ceremonies in the open-air birds nest stadium, the Chinese government seeded clouds with silver iodide to make it rain elsewhere. And there was no rain in Beijing for the opening events.

The Signal Corps Laboratories at Fort Monmouth were at the forefront of scientific exploration. What rain dances had been attempting to do for centuries, Fort Monmouth accomplished.

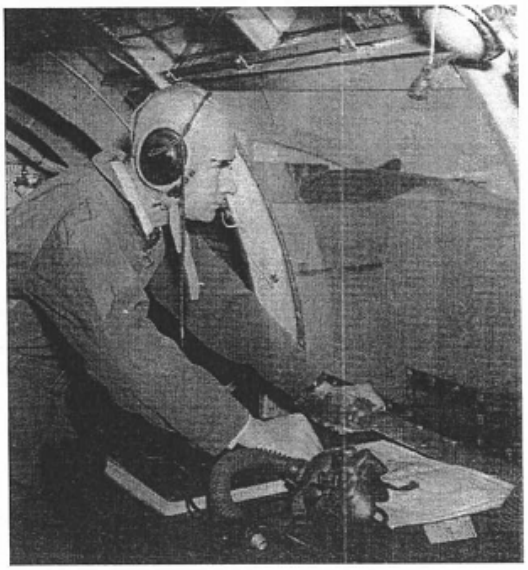

Dr. Vincent Schaefer prepares for a Project Cirrus flight in 1948.